Net Displacement and Temporal Scaling: Model Fitting, Interpretation, and Implementation

Garrett M. Street*[1], Tal Avgar[2], and Luca Börger[3]

[1]Department of Wildlife, Fisheries, and Aquaculture, Mississippi State University, Mississippi State, MS, 39762, USA

[2]Department of Integrative Biology, University of Guelph, Guelph, ON, N1G 2W1, Canada

[3]Department of Biosciences, College of Science, Swansea University, Swansea, SA2 8PP, United Kingdom

Manuscript type: Standard Paper.

Word count: 7027

Number of figures: 7

Number of tables: 1

*gms246@msstate.edu

Abstract

1. Net displacement is an integral component of numerous ecological processes and is critically dependent on the tortuosity of a movement trajectory and hence on the temporal scale of observation. Numerous attempts have been made to quantitatively describe net displacement while accommodating tortuosity, typically evoking a power law, but scale-dependency in tortuosity limits the utility of approaches based on power law relationships that must assume scale-invariant tortuosity.

2. We describe a phenomenological model of net displacement that permits both scale-variant and scale-invariant movement. Movement trajectories are divided into pairs of relocations specifying start- and end-points, and net displacements between points are calculated across a vector of time intervals. A bootstrap is implemented to create new datasets that are independent both across and within time intervals, and the model is fitted to the bootstrapped dataset using log-log regression. We apply this model to simulated trajectories and both fine-grain and coarse-grain trajectories obtained from a Aldabra giant tortoise (*Dipsochelys gigantea*), African elephants (*Loxodonta africana*), black-backed jackals (*Canis mesomelas*), and Northern elephant seals (*Mirounga angustirostris*).

3. The model was able to quantify the characteristics of net displacement from simulated movement trajectories corresponding to both scale-variant (e.g., correlated random walks) and scale-invariant (e.g., random walk) movement models. Further, the model produced identical outputs across time vectors corresponding to different intervals and absolute ranges of time for scale-invariant models. The model characterized the tortoise as generally exhibiting long scale-invariant steps, which was corroborated by visual comparison of model outputs to observed trajectories. Elephants, jackals, and seals exhibited movement parameters consistent with their known movement behaviors (nomadism, territoriality, and widely ranging searching).

4. We describe how the model may be used to compare movements within and between species, for example by partitioning movement into scale-variant and scale-invariant components, and by calculating a unitless net displacement scaled to the basal movement capacities of an animal. We also identify several useful derived quantities and realistic parameter ranges and discuss how the model may be implemented in a variety of ecological studies.

Keywords: bootstrap, fractal, movement, power law, random walk, regression, validation

Introduction

The displacement of animals over time is central to the developing field of movement ecology. Displacement is the distance between two positions along the movement path of an animal, and the resultant distance between the initial and final positions is called the net displacement. Net displacement increases with an animal's speed and with time but decreases with tortuosity ("sinuosity"), a measure of an animal's tendency to change its movement direction (Benhamou 2004; Rowcliffe *et al.* 2012; Turchin 2015). In the simplest scenario wherein movement is always forward (i.e., ballistic motion), net displacement is a positive linear function of time with the slope given by the animal's speed. Yet under the Random Walk paradigm, the expected net displacement increases with time but at a diminishing rate (Turchin 2015), leading to diffusive movement and thus a linear relationship between the squared net displacement and time. For any form of movement between ballistic and diffusive—for example, a correlated random walk—the relationship between expected net displacement and time will be determined by how tortuosity scales with time.

Numerous attempts have been made to quantitatively describe net displacement of animals while accommodating the tortuosity of the movement path (e.g., Williams 1992; Sanuy & Bovet 1997; Bergman *et al.* 2000). This is commonly addressed using a power law relationship wherein net displacement (R) changes as a function of sampling rate (hereafter refered to as temporal scale, τ) according to the power law relationship $R = a\tau^{1-\beta_1}$, where $a = e^{\beta_0}$, and β_0 and β_1 are the y-intercept and slope, respectively, estimated from the log-log regression of R against τ. In this formulation, $1 - \beta_1$ is the fractal dimension (D; Mandelbrot 1983). Fractal dimension has been widely used in ecological research as a supposedly scale-invariant measure of the tortuosity of a movement path (e.g., Weins *et al.* 1995; Nams 1996; Bascompte & Vilà 1997; Mårrell *et al.* 2002; Doerr & Doerr 2004; Nams 2005; Webb *et al.* 2009), with the coefficients a and D representing the length of a movement pathway at a standardized scale and the overall tortuosity of a movement path, respectively (Weins *et al.* 1995). This approach rests on the critical assumption that the

fractal dimension of a movement path is scale-independent ("self-similarity"; see Turchin 1996).

Hence, the critical assumption permitting the use of fractal dimension to describe the tortuosity of movement paths, and thus to estimate net displacement, is that tortuosity of animal movement is scale-independent (Turchin 1996; Schlägel & Lewis 2016). However, such may not be the case. At short temporal intervals (i.e., little time between animal relocations), animal movement tends to be decidedly linear—that is, turn angles (θ) tend to be small and favor forward movement [$\overline{\cos}(\theta) = 1$]; at longer intervals, movement tends toward highly tortuous movements [Brownian motion; $\overline{\cos}(\theta) = 0$]. The tortuosity of a movement path is thus highly scale-dependent, and net displacement depends on how tortuosity scales with time (Benhamou 2004; Turchin 1996; Rowcliffe *et al.* 2012; Schlägel & Lewis 2016). For example, Turchin (2015) demonstrated a decidedly non-linear decline in the natural logarithm of net displacement plotted against the natural logarithm of scale, and Benhamou (2004) found that the shape of this relationship is strongly dependent on the degree of directional persistence [i.e., $\overline{\cos}(\theta)$] in animal movement. These findings were empirically corroborated by Fritz *et al.* (2003), who described scale-dependence in fractal dimension using movement by wandering albatrosses (*Diomedea exulans*), and by Nams (2005), who used variation in fractal dimension to identify scales of perception in rodents. Thus estimating fractal dimension as a measure of tortuosity, and by extension assuming a scale-invariant power law relationship between net displacement and scale, could at best lead to artefactual results and at worst be completely misleading (Turchin 1996; Benhamou 2004; Turchin 2015). We could accommodate this consideration by allowing that τ scales to a function rather than a constant, but the *a priori* definition of the form of the scaling function and the relevant covariates will strongly influence the resulting model coefficients, and thus the inference achieved by modeling tortuosity. In summary, the appeal of the power law lies in its generality and applicability to a wide variety of theoretical scenarios, yet its dependence on scale-invariance limits its practical use.

This begs the questions: (i) how can we best model the relationship between net displacement and time, provided that tortuosity may be inconsistent across sampling intervals and hence

not scale-invariant? And, (ii) how would such a model be applied to real data for ecological inference? In light of these methodological difficulties, we posit that finding a phenomenological model of the relationship between net displacement and temporal scaling would permit meaningful comparisons between and within datasets and species. It would enable researchers to estimate the expected speed of an animal at any temporal resolution they wish, and could provide insight into encounter rates between agents, which are key issues in current ecological research (e.g., predator-prey, mates, individuals and cameras/traps, etc.; Avgar *et al.* 2011). Here we introduce such a model based on the decomposition of both scale-invariant and scale-variant components and demonstrate its application using both simulated and actual animal movement data. First, we define a model of net displacement permitting both scale-variant and -invariant tortuosity and describe its behavior under different parameterizations. We then simulate multiple movement trajectories under different movement strategies (random walk, biased random walk, and correlated random walk) at a constant step length. We use these data to evaluate the fit of the model, focusing on the ability of the model to capture the expectation in net displacement as a function of temporal scaling (i.e., the duration between consecutive relocations) for the different types of movement. Lastly, we apply the model to real animal movement data to further assess the inferential capabilities of the model using novel high temporal resolution continuous animal movement data obtained by dead-reckoning (i.e., sub-second relocation frequency) biologger data (Wilson *et al.* 2008), as well as low temporal resolution GPS-based relocation data (Abrahms *et al.* 2017).

Methods

Modeling net displacement

Our goal was to identify and evaluate a general model of net displacement permitting both scale-variant and -invariant tortuosity. We stress that our intention was not to construct a mechanistic model of the drivers of the relationship between temporal scale and spatial displacement (e.g.,

Van Moorter *et al.* 2009; Avgar *et al.* 2013a), but rather to provide a reliable phenomenological description of this relationship. Such a model would require only two inputs: a measure of displacement between two relocations (R), and the time elapsed between relocations (τ). Further, we wanted to develop our model from previous descriptions of net displacement following the power law, which enables the use of log-log regression to identify the scaling parameters of a model (Mandelbrot 1983; Weins *et al.* 1995; Turchin 2015). We thus defined our model as,

$$R_i = \tau_i^a e^{b\tau_i + c}, \tag{1}$$

which can be written as the log-log regression equation,

$$\ln R_i = a \ln \tau_i + b\tau_i + c + \epsilon_i, \tag{2}$$

where a and b are slopes and c an intercept estimated by log-log regression, ϵ is a normally distributed error term (i.e., $\epsilon \sim \mathrm{N}[0, \sigma]$), and τ is a vector of time intervals. This formulation requires $R_i > 0$ and $\tau_i > 0$. Here we consider τ a vector of integers satisfying $\tau = \kappa\{1, 2, \cdots, n\}$, where n is the number of time observations and κ is a scalar specifying the minimum time interval between observations (i.e., the temporal scale of relocations).

The inclusion of multiple slopes and an intercept deviates from previous attempts to model tortuosity (e.g., fractal dimension) and requires some interpretation. When $b = c = 0$, the model reduces to a simple geometric function $R = \tau^a$. This condition represents scale-invariant motion– that is, tortuosity does not change as a function of the scale of observation τ. The coefficient a is thus the slope of the log-linear relationship between τ (time) and R (displacement). The parameter b modifies the slope of the line as a multiplicative effect of τ, introducing skew to the relationship between R and τ as a function of τ. Specifically, $b > 0$ introduces positive skew to R at larger values of τ, and negative skew when $b < 0$ (Fig. S1). We thus term the parameter b the *skewness* of the log-linear slope a.

This functional form is robust in that when $b = 0$ fully scale-invariant tortuosity emerges (enabling identification of, for example, the fractal dimension D), but all other values of b add

curvature to R with increasing τ so as to permit a variety of possible realized forms of R (e.g., increasing with τ but at diminishing rates, concave/convex lines, etc.; Fig. S1). The values of a and b can produce marked differences in predicted R; however, limits to the range of these values can be set based on biological criteria. In the absence of local biases or periodic behaviors, the net displacement of a moving animal can only increase with time or remain constant (i.e., stationarity), so a must be greater than or equal to 0; however, the condition $a = 0$ (assuming $b = 0$) produces the nonsensical result of $R = 1$ across all values of τ. Further, we cannot conceive of a realistic scenario in which super-ballistic motion ($a > 1$) might emerge. We thus identify the practical range $0 < a \leq 1$ in the absence of periodic behaviors or local biases. Further, it is difficult to imagine a realistic scenario where speed may increase with τ (i.e., the derivative is non-positive for all positive τ), and as such the skewness b should be non-positive (0 inclusive). The condition $b < 0$ produces a decline in net displacement with time, facilitating identification of philopatric behaviors. The intercept c is a simple scaling parameter adjusting the basal velocity of the model to the scale of the data. As such, reorganizing the equation as $R' = R/e^c = \tau^a e^{b\tau}$ produces a unitless scaled net displacement such that when $\tau = 1$, $R' = e^b$ (i.e., net displacement is influenced only by the skewness). The value of c may be any real number ($-\infty < c < \infty$).

Simulating animal movement

To test the ability of the model to capture the relationship between net displacement and temporal scale, we first constructed 4 simple simulations of animal movement using classical random walk models representing both scale-variant and -invariant movement. We used four movement modes: (1) an uncorrelated random walk (i.e., Brownian motion; RW); (2 and 3) a correlated random walk with either narrow or wide dispersion in the distribution of turn angles (θ; CRWn and CRWw); and (4) and a random walk with local bias (i.e., a home range; BRW) based on a preferred heading toward a central location (i.e., [0,0]; see Online Supporting Information). In the random walk simulations, θ was sampled from a uniform distribution from 0 to 2π radians (RW), or from a wrapped Cauchy distribution with $\mu = 0$ and with the dispersion parameter

$\gamma = 0.2$ or 0.8 (CRWn and CRWw, respectively). For BRW, we defined $\gamma = 0.01$ as the Cauchy dispersion parameter of angular deviations from the direction of bias (the center of the home range). RW is a scale-invariant movement model, whereas CRWn and BRW are scale-variant models (Turchin 2015; Schlägel & Lewis 2016). Owing to extremely wide dispersion in turn angles but still generally correlated movement, CRWw represents an intermediate model between scale-variance and -invariance.

Second, we also constructed 4 simulations based on more complex movement rules: (1) central-place foraging (CPF); (2) a correlated random walk wherein the mover switches between exploratory (narrow dispersion in turn angles) and encamped (wide dispersion in turn angles) behaviors (i.e., a behaviorally composite model; cCRW); and (3 and 4) migration between 2 spatially discrete ranges wherein movement during the migratory phase is directed toward a seasonal center and movement during the residency phase is either a correlated random walk (mCRW) or a biased random walk (mBRW). In the CPF model, the mover proceeds in a random direction in a mostly linear fashion for a random number of time steps before being drawn to a constant spatial attractor (i.e., the "central place"). In the cCRW model, the distribution of turn angles alternates between $\gamma = 0.1$ (exploratory) and $\gamma = 0.9$ (encamped) depending on the behavioral state. In the mCRW and mBRW models, movements within sedentary ranges were parameterized as described above for CRW and BRW models, and movement toward the opposing seasonal center was directed as in the BRW model (see Online Supporting Information for more details). Step length (i.e., the distance between consecutive points) was set to a constant value of 1 for all simulations (i.e., movement always occurs). This prohibits the possibility of particularly long steps influencing the outcome of the modeling exercise and simplifies model evaluation.

Finally, the aforementioned simulations represent idealized movement trajectories following explicit rules for where an individual is likely to move based on its previous location and heading (and orientation relative to the direction of bias for biased walks); however, in reality animal movement is influenced by external factors such as food availability and abiotic condi-

tions (Nathan *et al.* 2008). Provided appropriate scaling parameters, a robust model should be capable of predicting net displacement regardless of whether movement is internally motivated by a simple mechanistic function (as above) or externally by the animal's environment. Thus for our final movement model we simulated a 2-resource landscape with spatially heterogeneous patches of resource availability (Fig. S2; simulations adapted from Matthiopoulos *et al.* 2015; see Online Supporting Information) and defined a simple RSF of the form,

$$\hat{Y} = 0.5X_1 + 2X_2. \tag{3}$$

The probability of selecting a given location in the landscape is the inverse-logit of the fitted values from the RSF (Fig. S2; Manly *et al.* 2002). We simulated movement on this landscape by basing movement on the probability of selection of cells within the von Neumann neighborhood with Manhattan distance $r = 2$ (i.e., 12 neighbors and a focal cell). We scaled the probability of selection for a given (x, y)-location such that $\sum_{i=1}^{13} P(x, y)_i = 1$. This Resource-Mediated Walk (RMW) model introduces three distinct differences from the previous models: (i) an individual has the option of not moving (i.e., $R = 0$); by extension, (ii) step lengths vary from 0 to r around a mean of 1.358; and, (iii) movement is not constrained to *a priori* definitions of turn angles and is determined by animal preference given the local landscape. In particular, the higher mean step length permits evaluation of the model's ability to capture differences in the base displacement capabilities of an animal. The landscape as parameterized here favors intense use of high probability locations punctuated by exploratory bouts due to its patchy nature, with certain areas strongly avoided (i.e., low-probability patches; Fig. S2). This means that at the scale of a step, movement is directed based on local habitat quality, which should be approximately random; at the scale of the landscape, movement should be structured based on broader landscape structure.

For each model we simulated 1,000,000 steps (Fig. 1). To construct a dataset of net displacement for a given model, we randomly selected a starting position at time t and identified the ending position at $t + \tau_i$. We calculated the net displacement between start and end positions for $\tau_i = \kappa i$ for $1 \leq i \leq 100$ and assuming $\kappa = 1$. We prohibited all time intervals from overlapping

to assure independence of observed values of R across values of τ. This procedure generates two vectors (τ and R) each of length $n = 100$, but the value of R at a given τ is determined by the random selection of the starting position. We thus repeated this procedure 100 times via a bootstrap to create a new dataset for each model, thereby increasing the amount of information available for analysis while ensuring independence between values of τ (see Online Supporting Information). We conducted log-log regressions of the form specified in Eqn. 2 to estimate a, b, and c for each individual bootstrapped dataset (i.e., 100 fitted models) assuming $\kappa = 1$ and defined the final model coefficients as the average of each coefficient across the individual models. We projected the exponentiated fitted values predicted by the final model coefficients across τ to visualize the predicted realized form of R. Finally, we repeated the bootstrap and model averaging procedures assuming $\kappa = 150$ to compare model outputs between time interval designations. All simulations and regressions were conducted using the `circular` and `base` packages in Program R v. 3.4.1 (R Core Team 2017).

Evaluating movement using empirical data

To evaluate the performance of our model with real animal movement data, we first used a high-frequency 12-day movement path dead-reckoned from GPS-corrected tri-axial accelerometer and magnetometer data recorded by a Daily Diary biologger affixed to the carapace of an Aldabra giant tortoise (*Dipsochelys gigantea*) on Round Island, Mauritius. Daily Diaries are multi-sensor biologging units comprising tri-axial accelerometer and magnetometer sensors (Wilson *et al.* 2008) which enable estimation of speed and orientation, respectively, at very high sampling frequency (here, 1 Hz), and allow reconstruction of fine-scale movements via dead reckoning (Wilson *et al.* 1991; Bidder *et al.* 2015). We used GPS locations to place the dead-reckoned track in real geographic space and to correct for the issue of error accumulation in dead-reckoned pathways (Bidder *et al.* 2015). These GPS locations were collected twice daily on the tortoise using a handheld high-precision GPS unit (Garmin GPSMAP 64s) following relocation of the animal using homing-in radiotracking using a Biotrack TW-5 twin-celled VHF tag also attached on the

carapace of the tortoise. Radiotracking was done using a Biotrack SIKARX8 Sika Receiver with a LINFLEX3 Lintec flexible 3-element Yagi antenna. All sensors and tags were placed inside housings attached to a baseplate affixed to the carapace of the animal using epoxy glue, and the combined weight of all tags was $< 3\%$ of the body weight of the animal. Given the slow rate of movement of the tortoise and the high frequency of relocation, this trajectory approximates the continuous movement path of the animal. We conducted the bootstrap and log-log regression modeling procedures described in *Simulating animal movement* on the resulting tortoise trajectory under three time interval scenarios ($\kappa = 1$, 50, and 100 seconds) to compare outputs given different temporal scaling rules.

We included a high-frequency dead-reckoned trajectory (fix rate of 1 Hz) as an idealized dataset approximating continuous movement, but such data are decidedly atypical for field studies of animal movements which often rely on relocations obtained via GPS at fix rates in units of minutes or hours rather than seconds. To demonstrate how this approach may be applied to typical GPS-based relocation data, we obtained the dataset reported by Abrahms *et al.* (2017). This dataset includes relocation data at a consistent 1-hour fix rate for multiple species and individuals within species. We selected 3 species to use for this analysis: a territorial carnivore (black-backed jackal, *Canis mesomelas*), a nomadic herbivore (African elephant, *Loxodonta africana*), and a highly mobile marine carnivore (Northern elephant seal, *Mirounga angustirostris*). Each species had 8-10 individuals each with a number of relocations $N \geq 5000$, or roughly 208 days at minimum. We performed the bootstrap and log-log regression analysis described in *Simulating animal movement* on each individual. Because of the smaller number of relocations for these animals relative to the tortoise, we restricted the length of the vector τ to $n = 80$ and defined $\kappa = 1$ hour.

Results

Characterizing simulated movement models

At $\kappa = 1$, the average net displacement R increased with the time interval τ in all simulated trajectories (Fig. 2), and the rate of increase a varied based on the movement strategy (Table 1). That a was not markedly different between 8 of the 9 models suggests that these trajectories exhibit predominately random motion. This is expected for RW and RMW, given the latter was dependent on a mostly random distribution of resources (Fig. S2). The CRWw simulation was parameterized to exhibit wide turn angles centered at 0, and despite a tendency toward forward motion this more closely resembled random movement. Similarly, the BRW simulation was generally spatially constrained, but again, the wide distribution of turning angles makes this model decidedly similar to random movement. The cCRW, mCRW, and mBRW simulations all had values of a between that of the RW and CRWn models, likely because of the behavioral switching characteristic of each; movement is more random in one behavioral mode and more directed in another, producing intermediate a-values. Conversely, the CRWn model exhibited mostly directed movement and thus produced the largest rate of increase. It also produced the largest negative value in skewness b (Table 1), implying a concave relationship between R and τ (i.e., R initially increases with τ, then decreases at very large values of τ beyond the range of fitted data). Our bootstrap approach allowed us to separately identify both the scale-invariant (a) and scale-variant (b) components of the CRWn model. The scaling parameter c was small in all simulations, suggesting little necessary scaling (as expected, given very small simulated step lengths).

At $\kappa = 150$, several model results were surprisingly consistent except those for CRWn, CPF, and both migratory models (Fig. 3). For CRWn, the magnitudes of a and b declined to the range of other models (Table 1), placing it at the value expected of a true random walk (i.e., $a = 0.5$ and $b = 0$). This is expected because, at very fine temporal scales (e.g., $\kappa = 1$), CRWn produces generally linear movements, but at broader scales (i.e., at scales exceeding the scale of correlation,

e.g., $\kappa = 50$) produces random motion. The CPF simulation produced the greatest difference in a at this magnitude of κ and actually exceeded the practical range identified in *Modeling net displacement* ($a = 1.2735$, Table 1); however, the range of τ specified by κ coupled to a negative skewness still resulted in a decline in predicted net displacement over time, consistent with philopatric behavior. Both migratory models produced reasonable values for a and b (Table 1), however their predicted net displacements accelerated across τ (Fig. 3). At this κ, start and end points for a randomly selected step are more likely to cross behavioral modes (i.e., sedentary vs. migratory) at larger values of τ, and the longer duration of these modes relative to those of the cCRW model resulted in much longer net displacements measured on average at larger τ.

Characterizing field movement data

The average net displacement R by the tortoise generally increased with τ (Fig. 4, bottom panels), but R exhibited structuring across τ due to frequent straight-line movements (Fig. 4, top panel). Regardless of the value of κ (i.e., the interval scalar for τ), this strongly directional movement resulted in a positive rate of increase a that exceeded the magnitude of a for all simulations (Table 1). The skewness b was decidedly small, suggesting scale-invariant movement over the duration of observation. The log-log regression explained 28% of the variation in net displacement for both values of κ, thus the majority of tortoise movement was driven by factors not considered by the model (e.g., environmental conditions, individual decisions by the animal, conspecific behavior, and/or error). All values of κ (1 s, 50 s, and 100 s, all high frequency time intervals for a tortoise) produced nearly identical models.

We also calculated R' (i.e., unitless net displacement scaled to the data) for the tortoise's bootstrapped dataset at $\kappa = 1$ and compared it to R' of the simulated datasets (Fig. 5). After scaling, the tortoise exhibited greater net displacement across all values of τ than did any simulation. This is due to the tortoise's strongly linear movements (Fig. 4, top panel) producing greater distance traveled relative to its absolute velocity (i.e., nearly ballistic motion), compared to the more random movements of the simulations (Fig. 1).

We repeated the analysis using the dataset of Abrahms *et al.* (2017). We observed remarkably little inter-individual variation in estimated model parameters (Fig. 6), with the greatest inter-individual variation occurring in the scaling parameter c (i.e., the intercept of the model). This suggests that individuals within species exhibit remarkably similar characteristics in movement. Conversely, each species exhibited unique average values across model coefficients. Jackals had the lowest log-linear slope (i.e., the scale-invariant component; $a = 0.71$) and the most strongly negative skewness (i.e., the scale-variant component; $b = -0.017$), indicative of more spatially-constrained movements consistent with territoriality. Elephants returned $a = 0.88$ and $b = -0.012$, indicating more directed movements at fine scales but similar skewness to jackals at broad scales (i.e., they traverse a broader range but have similar scale-dependent rates of decline in net displacement). Elephant seals had the largest log-linear slope and the weakest skewness ($a = 1.00$, $b = -0.003$). This indicates that at the finest scales measured (here, 1 hour) elephant seal movement is practically ballistic with concavity only occurring at broader temporal scales. Further, elephant seals also exhibited the largest values for the scaling parameter ($c = 7.20$), suggesting generally longer net displacements relative to jackals ($c = 5.03$) and elephants ($c = 5.66$).

It is noteworthy that the temporally coarse-scaled telemetry datasets produced comparable values of a to the tortoise and simulated trajectories, but consistently produced estimates of b that were 1–3 orders of magnitude larger than the temporally fine-scaled simulations and tortoise data (Fig. 6, middle row). This is consistent with the observation that animal movement shifts from directed movement at fine scales (e.g., $\kappa = 1$ second) toward tortuous movement at broad scales (e.g., $\kappa = 1$ hour), and reinforces that scale-dependence in net displacement should be expected across broad temporal windows.

Lastly, we calculated predicted values for R and R' for the telemetry datasets using the within-species average values for model coefficients across individuals (Fig. 7). Absolute net displacement for seals far exceeded that of elephants and jackals (Fig. 7, top panel), with seals moving 16.5 times farther than elephants after 80 hours on average, and 84.6 times farther than jack-

als. However, the magnitude of difference at larger values of τ was greatly diminished for R'. Scaled to the basal movement characteristics observed within each species (Fig. 7, bottom panel), the predicted R' of seals after 80 hours was only 3.5 times that of elephants, and 9.6 times that of jackals. This suggests that seals exhibit greater capacity for movement than do elephants or jackals, but the magnitude of difference in movement capacity is less profound (but still notably different) after accommodating inter-species differences in basal movement rates. That is, seals travel 16.5 times further in 80 hours than do elephants in terms of absolute distance, but after correcting for how quickly a seal moves relative to an elephant, the scaled distance is only 3.5 times greater.

Discussion

Tortuosity is an often scale-dependent phenomenon that complicates estimation of net displacement from an animal's movement trajectory. Here we identified a model incorporating the effect of time on observed net displacement acting through scale-dependency in tortuosity. The model enabled quantitative description of both scale-variant (CRWn, CRWw, BRW, CPF, cCRW, mCRW, and mBRW) and scale-invariant models of net displacement (RW, RMW), and was insensitive to differences in the time lag over which the model was estimated for the tortoise, potentially due to the high sampling frequency represented by our values of κ. The model applied equally to both large (i.e., simulations and tortoise data) and small (i.e., GPS-based telemetry) relocation datasets. Further, we developed a bootstrap framework for creating independent data to fit the model to temporally autocorrelated movement trajectories. This work builds on previous studies describing how tortuosity of movement changes across temporal scales (e.g., Fritz *et al.* 2003; Benhamou 2004; Turchin 2015) and provides a novel and informative platform for ecological inference from movement trajectories.

A merit of this modeling approach is the ability to partition animal movement into scale-invariant and scale-variant components based on observed movement trajectories. The log-linear

slope a of our model is determined by directional persistence; an animal that typically moves in straight lines with very little tortuosity will exhibit values of a approaching 1, whereas a approaches 0 as movement becomes more spatially constrained within a geographic region. The net displacement predicted by τ^a assumes scale-invariant tortuosity (Benhamou 2004; Turchin 2015), thus τ^a represents the scale-invariant component of a movement trajectory. Conversely, $e^{b\tau+c}$, by virtue of applying skewness to scale-invariant motion, represents the scale-variant component of an observed trajectory. The degree of directional persistence that remains after controlling for scale-variant movement may thus be estimated directly from the model. This enables direct comparison of directional persistence between individuals or species, or with respect to different spatiotemporal windows. As such the quantity τ^a is proportional to the rate of dispersal over a given time interval, depressed by scale-variance ($e^{b\tau+c}$).

The expected net displacement, R, is the primary output of the model and can be used to predict how far an animal is likely to travel in a finite amount of time τ. However, when $\tau = 1$, the scale-invariant component of the model reduces to 1, and the remaining scale-variant component e^{b+c} produces a net displacement from the base movement capacity of the animal. The quantity e^{b+c} is thus the linear speed v of the animal based on the observed movement trajectory measuring the distance traveled at the smallest time interval possible (i.e., $\tau = 1$). For example, our simulated movers exhibited linear speeds as predicted by the final models at $\kappa = 1$ of $v_{RW} = 0.8035$, $v_{BRW} = 0.8150$, $v_{CRWn} = 1.2177$, $v_{CRWw} = 0.9150$, and $v_{RMW} = 1.3347$. These compare favorably with our model parameterization procedures where the distance between consecutive steps was 1 linear unit for RW, BRW, CRWn, and CRWw, and the expected distance was 1.38 linear units for RMW (i.e., the 95% quantiles generated by the bootstrap always included the expected linear step length, a finding that was consistent across both values of κ). Further, our tortoise exhibited $v_{\kappa=1} = 0.0005$ m/s, $v_{\kappa=50} = 0.0006$ m/s, and $v_{\kappa=100} = 0.0006$ m/s, indicating that our approach can reliably extract the linear speed from a movement dataset at different ranges and intervals of τ. It should be noted that the movement observed in the dataset produces the calculated linear speed, and this speed does not necessarily correspond to

390 the basal movement speed an animal is capable of assuming (e.g., its maximum or minimum velocity); rather, it is an estimate of central tendency in the basal movement capacity of the animal. However, our estimates of v_κ were close to the observed median velocity of the tortoise 393 ($v = 0.0003$ m/s), suggesting the model is capable of reliably extracting the linear speed of the animal. Multiplication of the linear speed by a time interval τ_i enables calculation of the cumulative distance d (in contrast to the net displacement R) the animal is likely to travel over 396 that time interval. For example, an animal with a linear speed of 1 linear unit per time unit, over 10 time units, will have traveled $d = 10$ linear units. Estimates of absolute distance traveled are generally biased low due to tortuosity, and having a method by which to estimate total 399 distance traveled is recognized as a critical research front (Rowcliffe *et al.* 2012). This may be particularly useful from an energetics perspective, where net energy expenditure is expected to correlate strongly with d and may be compared across landscapes of variable quality and energy 402 availability.

Further, the total distance traveled d may be compared to the realized net displacement R as a ratio describing the tortuosity of the animal's trajectories (a.k.a., the straightness index). Being a 405 ratio, this is a unitless estimate that may be compared between groups to examine a wide variety of ecological phenomena. For example, the tortuosity of an animal's movement trajectory is a primary determinant of the rate of diffusion (Turchin 2015), which has direct implications for 408 the dispersal capabilities of an organism and the rate at which it traverses its occupied space (e.g., Doerr & Doerr 2004; Webb *et al.* 2009). It may be an indicator of habitat quality, with more tortuous movements occurring in high quality areas as animals increase their searching efforts 411 (Morales *et al.* 2004; Fryxell *et al.* 2008), or in response to barriers and perceived risk (Whittington *et al.* 2004; Avgar *et al.* 2013b). Tortuosity produces a net increase in energetic expenditure, producing a trade-off between movement efficiency and searching efficacy that should influence 414 the directional persistence of a movement trajectory (Wilson *et al.* 2013). This in turn implies a fitness cost to searching and habitat selection driven by tortuosity at the individual level, which consequently influences the dynamics and stability of an entire population (Matthiopoulos *et al.*

2015). As such, the magnitude of tortuosity and its ecological influence may be inconsistent across both spatial (e.g., Fritz *et al.* 2003; Fryxell *et al.* 2008; Webb *et al.* 2009; Turchin 2015) and temporal scales (Benhamou 2004; Matthiopoulos *et al.* 2015; Turchin 2015), and this inconsistency may have profound implications for seasonal migrations, population dynamics, and species distributions over space and time. Our approach offers a flexible and robust method to estimate tortuosity across spatiotemporal scales, providing a new window through which to view these issues.

Similarly, we may draw comparisons between groups or individuals in terms of the linear speed, which should be expected to vary with respect to, for example, landscape permeability, the spatial orientation and configuration of barriers to movement, and the movement medium (e.g., land vs. water; see Figs. 6 & 7). However, linear speed as estimated here is particularly interesting when considered from the perspective of allometry. A common finding in studies of ecological scaling is that numerous phenomena tend to scale with animal body mass. Classically this has focused on the scaling of metabolic rate, and now what is collectively recognized as the metabolic theory of ecology (Brown *et al.* 2004) is generally considered to influence or directly govern numerous ecological processes including life history characteristics, population dynamics, biomass production, trophic dynamics, and individual fitness. Given the well-documented body size dependency of the components of animal gait (e.g., stride length and frequency; McMahon 1975), it is conceivable that an animal's intrinsic movement capabilities could also consistently scale with body mass. We thus expect the linear speed to be proportional to body mass at a scale of 0.75, consistent with metabolic theory (i.e., $e^{b+c} = \gamma M^{0.75}$; Brown *et al.* 2004).

Our model structure also offers inferential flexibility in terms of quantities that may be derived from the fitted model. For example, the derived value $-a/b$, provided $b < 0$, is the "tipping point" of the model and identifies the time interval necessary to achieve the maximum net displacement. From a behavioral perspective, this quantity could correspond to the amount of time required for an animal to traverse its home range, which we denote as τ_{HR}. This requires investigation with more data than we currently have available, but if this is the case, the quantity $R_{HR} = \tau_{HR}^{a} e^{b\tau_{HR}+c}$ will be proportional to the linear home range size of the animal. This rela-

tionship permits investigation of the rate of home range traversal R_{HR}/τ_{HR} with respect to, for example, conspecific density (particularly relevant for territorial species), resource availability, or seasonality. However, we stress that calculation of R_{HR} will require extrapolating outside the range of data used to fit the model when $\tau_{HR}/\kappa > n$ (the maximum number of intervals between observations), and R_{HR} should be treated as a hypothetical outcome to be tested rather than a definite conclusion.

The scaled net displacement R' is another useful derived value enabling direct comparison of net displacement between animals with markedly different linear speeds (Figs. 5 & 7). Here we may examine, for example, how far different animals travel with respect to their basal movement rates. This may have profound implications for individual- or species-specific partitioning of energy or effort, which in turn permits investigation of the relative contribution of animal movement to net fitness. In some circumstances, we may find that a slow moving animal, such as our tortoise, may in fact outpace faster organisms at the scale of their average linear speed. (The tortoise may indeed be faster than the hare at their respective scales of movement!) Alternatively, we could compare R' within a species across landscapes to assess how net displacement covaries with landscape structure and composition, or within a single animal or species provided some partitioning of the movement trajectory into relevant bins. For example, the characteristics of animal movement will likely vary between exploratory (dispersive) and encamped (home-ranging) movements (Morales *et al.* 2004; Fryxell *et al.* 2008). Application of this approach to these discrete movement categories may reveal trends in the scaling of net displacement, the linear speed, or directional persistence as a function of both the movement mode and associated landscape characteristics. This would be useful to create mechanistic models of animal movement based on the most likely parameterization of our model, provided a means to relate the behavioral state to spatiotemporal covariates (e.g., a switching state-space model; Morales *et al.* 2004). This in turn could provide new insight into the drivers of space use, which are known to vary based on complicated interactions with biotic and abiotic conditions and spatiotemporal scales (e.g., Fritz *et al.* 2003; Fryxell *et al.* 2008; Street *et al.* 2016; Prokopenko *et al.* 2017). However, note that

comparisons of the fitted predictions of R' require identical values of κ for each set of predictions (see Figs. 5 & 7), otherwise predictions may occur over vastly different temporal windows and resolutions.

We found that our modeling approach produced nearly identical models of net displacement by the tortoise across markedly different ranges of τ (Table 1). This indicates that our modeling approach was insensitive to the absolute magnitude and range of τ over this period of the animal's movement. Rather than being an indication of model robustness to the range and intervals of τ (considering that $\kappa = 1$, 50, and 100 are still high-frequency samples for tortoise), we interpret this as an indicator that the animal's general movement strategy (characterized by particular values of a, b, and c) did not change over that time period. This may assist determination of whether the movement behavior of the animal is consistent over the period under observation. Differences in estimated model parameters as determined by, for example, a Z-score (e.g., $Z = (\beta_{1,\text{model}\,1} - \beta_{1,\text{model}\,2}) / \sqrt{\sigma^2_{\beta_1} + \sigma^2_{\beta_2}}$) would constitute evidence that the animal experienced a change in behavior during the period encompassed by the larger values of $\kappa\tau$. The point in time in which a change occurred could then be identified by, for example, a switching state-space model (Morales *et al.* 2004), piecewise regression (Toms & Lesperance 2003), or breakpoint analysis (Lavielle & Teyssiére 2006), and separate models could be fit to periods of different behavior to draw comparisons between movement strategies as described earlier. Estimated model parameters may be similarly compared to parameters that are known analytically for certain movement strategies (e.g., $a = 0.5$ for a random walk; Turchin 2015).

The practical application of this model will necessitate identification of values of κ (the time interval between observations) and n (the number of observations) appropriate to the amount of data available—that is, given a number of animal relocations (N), what values should one assign to κ and n? First, note that κ is minimally restricted by the fix rate between observations; if relocations are recorded once per hour as in the telemetry data used here (Abrahms *et al.* 2017), κ cannot be less than 1 hour. Maximally, κ is restricted by the total time elapsed in the dataset (T). When $\kappa = T$, n can only be 1; when $\kappa \approx N/3$, the maximum value of n increases to 2. Consider

that for the i-th element in the vector τ we make $i+1$ points unavailable for later selection in the bootstrap to ensure independence (the start and end points, and all points between), thus at $i = n$ we have removed a total of $\sum_{i=1}^{n}(i+1) = \sum_{i=1}^{n} i + n$ observations from potential selection. By adding the κ constant and invoking the rule of summation, we arrive at $N \geq \kappa\frac{n(n+1)}{2} + n$, and we can define the function $f(N,\kappa) = \lfloor \frac{-(\frac{\kappa}{2}+1)+\sqrt{(\frac{\kappa}{2}+1)^2+2\kappa N}}{\kappa} \rfloor$ as the maximum n permissible provided κ and N (based on the above summation, the quadratic formula, and the greatest integer function). We may also define the function $f(N,n) = \lfloor \frac{2N}{n(n+1)} - \frac{2}{n+1} \rfloor$ as the maximum κ permissible provided n and N. These functions provide the maximum values of κ and n under optimal conditions, but due to the random nature of the bootstrap these values will likely not be achievable in practice. We provide these functions as upper limits to the parameters but κ and n should be set to lower values than these to accommodate the bootstrap. We also advise selecting data for the largest values of τ first to facilitate random data selection (see Online Supporting Information).

Lastly, our approach as described assumes consistency in the fix rate across the dataset. What if this assumption is violated, for example because numerous gaps occur in the dataset? This is a common problem across studies of animal movement, and our approach as described does assume consistency in the fix rate. One common solution to such a scenario would be to subsample the relocations to a consistent fix rate (see for example Abrahms *et al.* 2017), but this may not accommodate all scenarios where, for example, there may be a gap in relocations of multiple days or weeks in an otherwise fine-scale dataset. In that case, one would simply require that the difference in the timestamps of the start and end points of the i-th randomly selected step satisfies the temporal gap specified by $\kappa\tau_i$. If this rule is not met, a different start- and end-point set would be selected until the rule is satisfied. This would likely also require additional attention to values of n and κ as described above.

In conclusion, there is much to be gained from characterizing and understanding the net displacement of animals. We presented a phenomenological model that enables characterization of net displacement under both scale-variant and scale-invariant movement strategies. This facil-

itates graphical evaluation of net displacement across a gradient of temporal scale, and model parameters may be compared across individuals, species, landscapes, and bioclimatic gradients to assess the ecological drivers of net displacement and tortuosity. They may also be used to characterize the relative contribution of scale-variant and scale-invariant movement to realized net displacement and movement trajectories. Further, numerous derived quantities from the model may be used to explore a wide variety of ecological phenomena, including habitat quality, rates of dispersal, home ranging, partitioning of effort, and energetic and allometric scaling relationships, as well as how they contribute to, and are influenced by, variation in movement. Our model thus represents a quantitative link between the the movements of individuals and numerous ecological processes and fields.

Acknowledgments

We thank S. F. Oppenheimer for discussion of identification of parameter upper limits. This work was funded partly by the Mississippi State University Office of Research and Economic Development, and the Mississippi State University Forest and Wildlife Research Center. We thank Durrell Conservation Trust for funding and support of the tortoise data. J. Redcliffe collected the tortoise data and dead-reckoned the track; J. Redcliffe, L. Borger, N. Cole, and Mauritian Wildlife Foundation organised and supported the field work. Permits and ethical guidelines were provided by Durrell Conservation Trust, Mauritius Wildlife Foundation, and the College of Science, Swansea University.

Data Accessibility

Simulated movement trajectories were created using the R code supplied in the online Supporting Information. Tortoise data is available upon request to LB. Telemetry data from Abrahms *et al.* (2017) is available on MoveBank.

References

549 Abrahms, B., Seidel, D.P., Dougherty, E., Hazen, E.L., Bograd, S.J., Wilsom, A.M., McNutt, J.W., Costa, D.P., Blake, S., Brashares, J.S. & Getz, W.M. (2017) Suite of simple metrics reveals common movement syndromes across vertebrate taxa. *Movement Ecology*, **5**, 12.

552 Avgar, T., Deardon, R. & Fryxell, J.M. (2013a) An empirically parameterized individual based model of animal movement, perception, and memory. *Ecological Modelling*, **82**, 158–172.

Avgar, T., Kuefler, D. & Fryxell, J.M. (2011) Linking rates of diffusion and consumption in relation
555 to resources. *American Naturalist*, **178**, 182–190.

Avgar, T., Mosser, A., Brown, G.S. & Fryxell, J.M. (2013b) Environmental and individual drivers of animal movement patterns across a wide geographical gradient. *Journal of Animal Ecology*,
558 **251**, 96–106.

Bascompte, J. & Vilà, C. (1997) Fractals and search paths in mammals. *Landscape Ecology*, **12**, 213–221.

561 Benhamou, S. (2004) How to reliably estimate the tortuosity of an animal's path: straightness, sinuosity, or fractal dimension? *Journal of Theoretical Biology*, **229**, 209–220.

Bergman, C.M., Schaefer, J.A. & Luttich, S.N. (2000) Caribou movement as a correlated random
564 walk. *Oecologia*, **123**, 364–374.

Bidder, O.R., Walker, J.S., Jones, M.W., Holton, M.D., Urge, P., Scantlebury, D.M., Marks, N.J., Magowan, E.A., Maguire, I.E. & Wilson, R.P. (2015) Step by step: reconstruction of terrestrial
567 animal movement paths by dead-reckoning. *Movement Ecology*, **3**, 23.

Brown, J.H., Gillooly, J.F., Allen, A.P., Savage, V.M. & West, G.B. (2004) Toward a metabolic theory of ecology. *Ecology*, **85**, 1771–1789.

570 Doerr, V.A.J. & Doerr, E.D. (2004) Fractal analysis can explain individual variation in dispersal search paths. *Ecology*, **85**, 1428–1438.

Fritz, H., Said, S. & Weimerskirch, H. (2003) Scale-dependent hierarchical adjustments of movement patterns in a long-range foraging seabird. *Proceedings of the Royal Society Series B: Biological Sciences*, **270**, 1143–1148.

Fryxell, J.M., Hazell, M., Börger, L., Dalziel, B.D., Morales, J.M., McIntosh, T. & Rosatte, R.C. (2008) Multiple movement modes by large herbivores at multiple spatiotemporal scales. *Proceedings of the National Academy of Sciences of the United States of America*, **49**, 19114–19119.

Lavielle, M. & Teyssiére, G. (2006) Détection de ruptures multiples dans des séries temporelles multivariées. *Lietuvos Matematikos*, **46**, 25.

Mandelbrot, B.B. (1983) *The Fractal Geometry of Nature*. W. H. Freeman, San Francisco, CA.

Manly, B.F.J., McDonald, L.L., Thomas, D.L., McDonald, T.L. & Erickson, W.P. (2002) *Resource Selection by Animals: Statistical Design and Analysis for Field Studies*. Kluwar Academic Publishers, Dordrecht, The Netherlands, 2 edition.

Mårrell, A., Ball, J.P. & Hofgaard, A. (2002) Foraging and movement paths of female reindeer: insight from fractal analysis, correlated random walks and lévy flights. *Canadian Journal of Zoology*, **80**, 854–865.

Matthiopoulos, J., Fieberg, J., Aarts, G., Beyer, H.L., Morales, J.M. & Haydon, D.T. (2015) Establishing the link between habitat selection and animal population dynamics. *Ecological Monographs*, **85**, 413–436.

McMahon, T.A. (1975) Using body size to understand the structural design of animals: quadrupedal locomotion. *Journal of Applied Physiology*, **39**, 619–627.

Morales, J.M., Haydon, D.T., Frair, J., Holsinger, K.E. & Fryxell, J.M. (2004) Extracting more out of relocation data: building movement models as mixtures of random walks. *Ecology*, **85**, 2436–2445.

Nams, V.O. (1996) The VFractal: a new estimator for fractal dimension of animal movement paths. *Landscape Ecology*, **11**, 289–297.

Nams, V.O. (2005) Using animal movement paths to measure response to spatial scale. *Oecologia*, **143**, 179–188.

Nathan, E., Getz, W.M., Revilla, E., Holyoak, M., Kadmon, R., Saltz, D. & Smouse, P.E. (2008) A movement ecology paradigm for unifying organismal movement research. *Proceedings of the National Academy of Sciences of the United States of America*, **105**, 19052–19059.

Prokopenko, C.M., Boyce, M.S. & Avgar, T. (2017) Characterizing wildlife behavioural responses to roads using integrated step selection analysis. *Journal of Applied Ecology*, **54**, 470–479.

R Core Team (2017) *R: A Language and Environment for Statistical Computing*. R Foundation for Statistical Computing, Vienna, Austria.

Rowcliffe, J.M., Carbone, C., Kays, R., Kranstauber, B. & Jansen, P.A. (2012) Bias in estimating animal travel distance: the effect of sampling frequency. *Methods in Ecology and Evolution*, **3**, 653–662.

Sanuy, D. & Bovet, P. (1997) A comparative study on the paths of five anura species. *Behavioural Processes*, **41**, 193–199.

Schlägel, U.E. & Lewis, M.A. (2016) A framework for analyzing the robustness of movement models to variable step discretization. *Journal of Mathematical Biology*, **73**, 815–845.

Street, G.M., Fieberg, J., Rodgers, A.R., Carstensen, M., Moen, R., Moore, S.A., Windels, S.K. & Forester, J.D. (2016) Habitat functional response mitigates reduced foraging opportunity: implications for animal fitness and space use. *Landscape Ecology*, **31**, 1939–1953.

Toms, J.D. & Lesperance, M.L. (2003) Piecewise regression: a tool for identifying ecological thresholds. *Ecology*, **84**, 2034–2041.

618 Turchin, P. (1996) Fractal analyses of animal movement: a critique. *Ecology*, **77**, 2086–2090.

Turchin, P. (2015) *Quantitative Analysis of Movement: Measuring and Modeling Redistribution in Animals and Plants*. Beresta Books, Mansfield, CT, 2 edition.

621 Van Moorter, B., Visscher, D., Benhamou, S., Börger, L., Boyce, M.S. & Gaillard, J.M. (2009) Memory keeps you at home: a mechanistic model for home range emergence. *Oikos*, **118**, 641–652.

624 Webb, S.L., Riffell, S.K., Gee, K.L. & Demarais, S. (2009) Using fractal analyses to characterize movement paths of white-tailed deer and response to spatial scale. *Journal of Mammalogy*, **90**, 1210–1217.

627 Weins, J.A., Crist, T.O., With, K.A. & Milne, B.T. (1995) Fractal patterns of insect movement in microlandscape mosaics. *Ecology*, **76**, 663–666.

Whittington, J., St. Clair, C.C. & Mercer, G. (2004) Path tortuosity and the permeability of roads
630 and trails to wolf movement. *Ecology and Society*, **9**, 4.

Williams, B. (1992) The measurement of "sinuosity" in correlated random walks. *Journal of Theoretical Biology*, **155**, 437–442.

633 Wilson, R.P., Griffiths, I.W., Legg, P.A., Friswell, M.I., Bidder, O.R., Halsey, L.G., Lambertucci, S.A. & Shepard, E.L.C. (2013) Turn costs change the value of animal search paths. *Ecology Letters*, **16**, 1145–1150.

636 Wilson, R.P., Shepard, E.L.C. & Liebsch, N. (2008) Prying into the intimate details of animal lives: use of a daily diary on animals. *Endangered Species Research*, **4**, 123–137.

Wilson, R.P., Wilson, M.P.T., Link, R., Mempel, H. & Adams, N.J. (1991) Determination of move-
639 ments of african penguins *spheniscus demersus* using a compass system: dead reckoning may be an alternative to telemetry. *Journal of Experimental Biology*, **157**, 557–564.

Tables

Table 1: Average log-log regression outputs for simulated animal movement models and Aldabra giant tortoise (*Dipsochelys gigantea*) relocations

κ	Dataset	a	SE_a	b	SE_b	c	SE_c	R^2
1	RW	0.4743	0.0140	0.0008	0.0005	-0.2196	0.0356	0.35
	BRW	0.4643	0.0139	0.0008	0.0004	-0.2054	0.0322	0.35
	CRWn	0.7038	0.0103	-0.0036	0.0004	0.2005	0.0188	0.48
	CRWw	0.4926	0.0150	0.0004	0.0005	-0.0893	0.0352	0.35
	RMW	0.4313	0.0110	0.0005	0.0004	0.2883	0.0238	0.31
	CPF	0.4696	0.0210	0.0042	0.0008	-0.1696	0.0417	0.23
	cCRW	0.5444	0.0143	-0.0010	0.0006	-0.0656	0.0301	0.27
	mCRW	0.5998	0.0199	-0.0005	0.0007	-0.2104	0.0414	0.25
	mBRW	0.5196	0.0219	-0.0004	0.0008	-0.1118	0.0447	0.17
150	RW	0.4832	0.0164	0.000008	0.000004	-0.1964	0.1166	0.34
	BRW	0.4590	0.0169	-0.00002	0.000004	-0.0574	0.1213	0.20
	CRWn	0.4891	0.0122	0.00001	0.000003	-0.9018	0.0868	0.39
	CRWw	0.5250	0.0167	-0.00002	0.000003	-0.2571	0.1216	0.30
	RMW	0.3762	0.0175	0.000001	0.000004	0.6619	0.1235	0.16
	CPF	1.2735	0.0248	-0.0002	0.000005	-3.7947	0.1870	0.33
	cCRW	0.5707	0.0193	-0.00002	0.000004	-0.3622	0.1424	0.41
	mCRW	0.9369	0.0284	-0.00008	0.000005	-2.4946	0.2087	0.47
	mBRW	0.7988	0.0373	0.000001	0.000007	-2.4208	0.2709	0.39
1	Tortoise	0.9541	0.0355	0.0007	0.0011	-7.6215	0.0826	0.27
50		0.9569	0.0384	0.00002	0.00003	-7.3843	0.2354	0.28
100		0.9569	0.0380	-0.000005	0.00001	-7.4368	0.2626	0.28

Note: RW = Random Walk; BRW = Biased Random Walk; CRWn = Correlated Random Walk with narrow dispersion of turn angles; CRWw = Correlated Random Walk with wide dispersion of turn angles; RMW = Resource-Mediated Walk; CPF = Central-Place Foraging; cCRW = composite Correlated Random Walk; mCRW = migratory Correlated Random Walk; mBRW = migratory Biased Random Walk; Tortoise = tortoise relocation data; a = slope of the log-log relationship between R and δ; b = skewness of the slope; c = scaling parameter; κ = time interval between observations.

Figure captions

Figure 1: Simulated trajectories from 9 movement strategies. Turn angles were sampled from a uniform distribution from 0 to 2π radians (Random Walk), or from a wrapped Cauchy distribution with $\mu = 0$ and $\gamma = 0.2$, 0.8, and 0.01 (Correlated Random Walk with narrow or wide dispersion, and Biased Random Walk), with a constant step length (i.e., at $\tau = 1$, $R = 1$). In the Resource-Mediated Walk, movement was driven by the probability of selecting a cell based on a hypothetical Resource Selection Function within the von Neumann neighborhood of Manhattan distance $r = 2$.

Figure 2: Bootstrapped data of net displacement (R) from 9 simulated movement trajectories across time intervals (τ) assuming $\kappa = 1$. Expected net displacement (black line) is calculated from the function $R = \tau^a e^{b\tau+c}$.

Figure 3: Bootstrapped data of net displacement (R) from 9 simulated movement trajectories across time intervals (τ) assuming $\kappa = 150$. Expected net displacement (black line) is calculated from the function $R = \tau^a e^{b\tau+c}$.

Figure 4: Movement trajectory of an Aldabra giant tortoise (*Dipsochelys gigantea*) projected in UTM Zone 40 (m), associated bootstrapped data net displacement (R) across time intervals (τ) at different sampling intervals ($\kappa = \{1, 50, 100\}$), and expected net displacement (black line) calculated from the function $R = \tau^a e^{b\tau+c}$.

Figure 5: Net displacement scaled to the movement capacity inherent to each dataset ($R' = \tau^a e^{b\tau}$) for simulated trajectories and for Aldabra giant tortoise (*Dipsochelys gigantea*) data at $\kappa = 1$.

Figure 6: Bootstrap model results of the form $R = \tau^a e^{b\tau+c}$ using 1-hour resolution GPS relocation data for African elephants (*Loxodonta africana*), Northern elephant seals (*Mirounga angustirostris*), and black-backed jackal (*Canis mesomelas*). Intervals are the 95% empirical confidence intervals obtained from the bootstrapped distribution. Values along x-axis are the last 1 or 2 digits of the animal identification code in the dataset reported by Abrahms *et al.* (2017).

Figure 7: Predicted absolute net displacement ($R = \tau^a e^{b\tau+c}$, top panel) and net displacement scaled to the basal movement rate of the species ($R' = \tau^a e^{b\tau}$, bottom panel) using 1-hour resolution GPS relocation data for African elephants (*Loxodonta africana*), Northern elephant seals (*Mirounga angustirostris*), and black-backed jackal (*Canis mesomelas*).

648

Figure 1

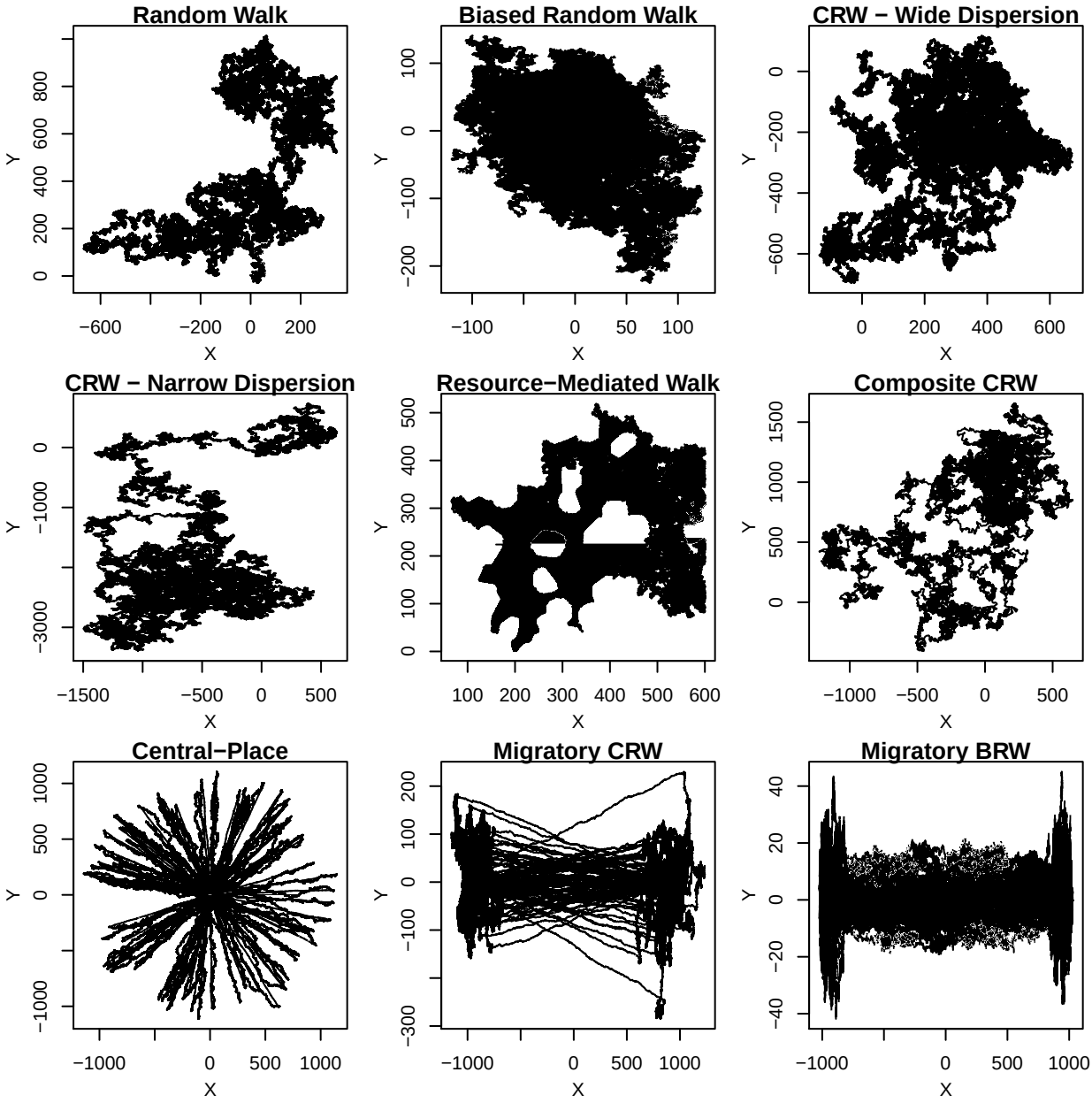
Random Walk
Biased Random Walk
CRW − Wide Dispersion
CRW − Narrow Dispersion
Resource−Mediated Walk
Composite CRW
Central−Place
Migratory CRW
Migratory BRW
X
Y

Figure 2

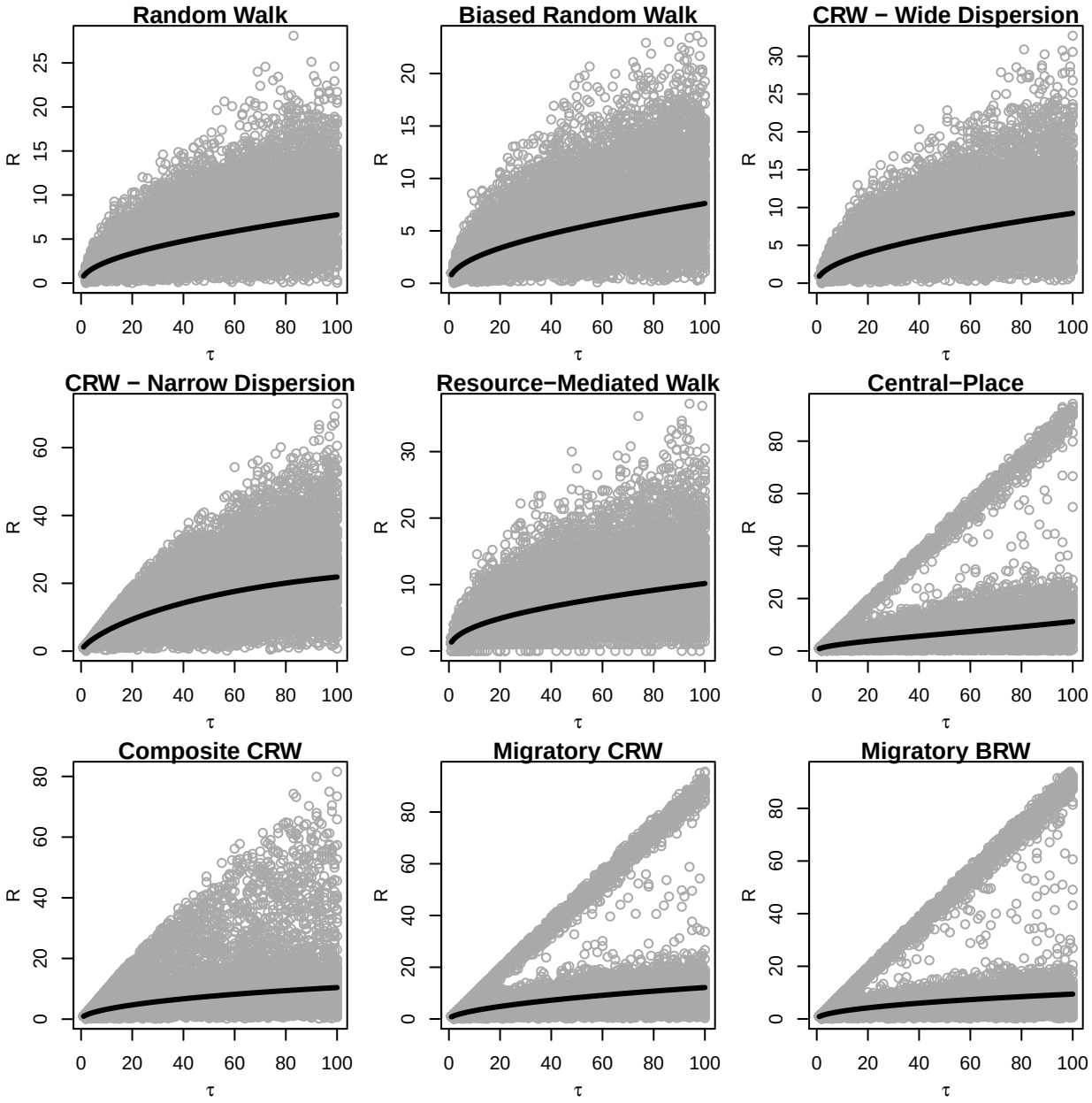
Random Walk
Biased Random Walk
CRW − Wide Dispersion
CRW − Narrow Dispersion
Resource−Mediated Walk
Central−Place
Composite CRW
Migratory CRW
Migratory BRW
R
τ

Figure 3

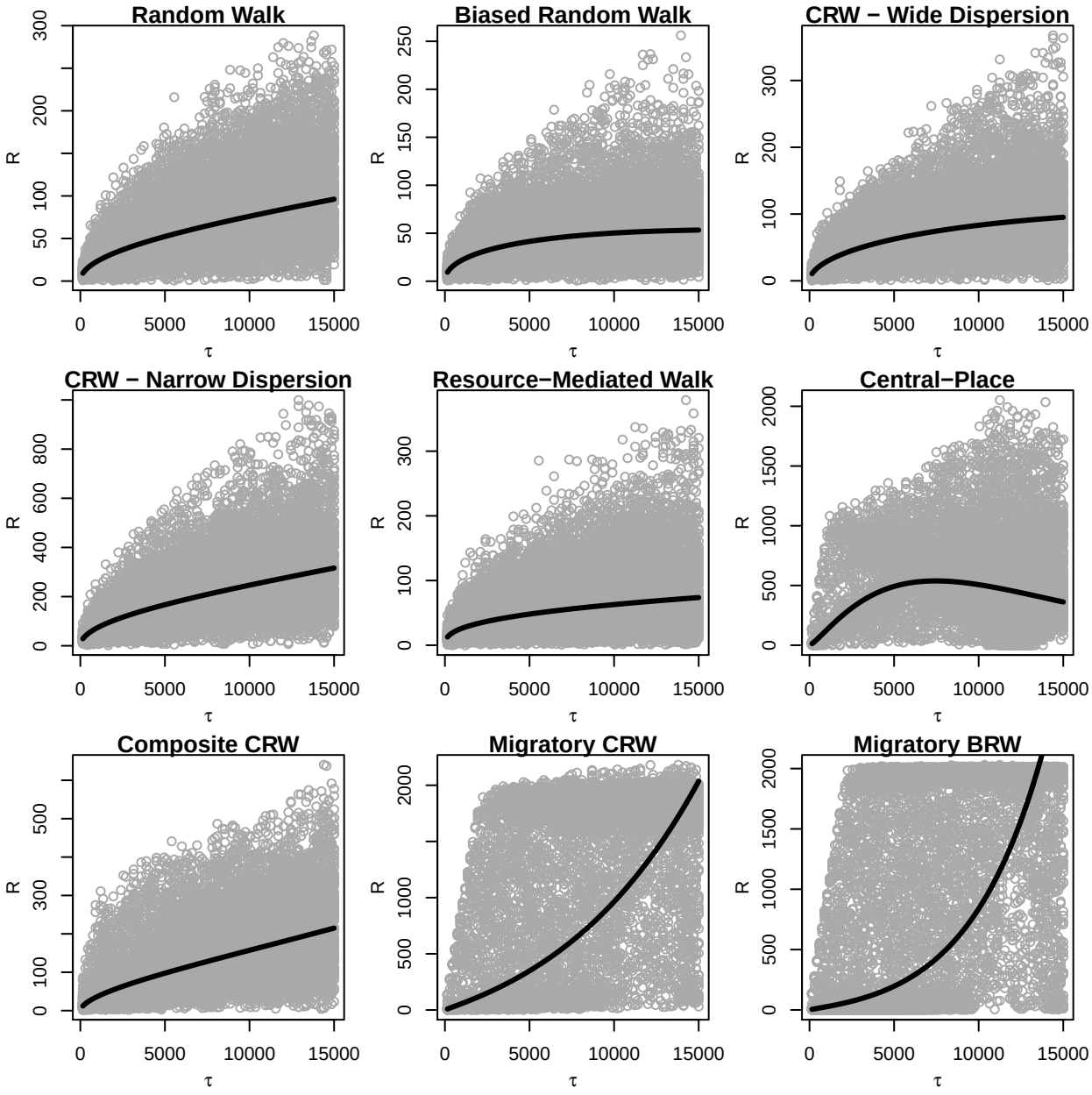
Random Walk
Biased Random Walk
CRW − Wide Dispersion
CRW − Narrow Dispersion
Resource−Mediated Walk
Central−Place
Composite CRW
Migratory CRW
Migratory BRW
R
τ
0
5000
10000
15000

651

Figure 4

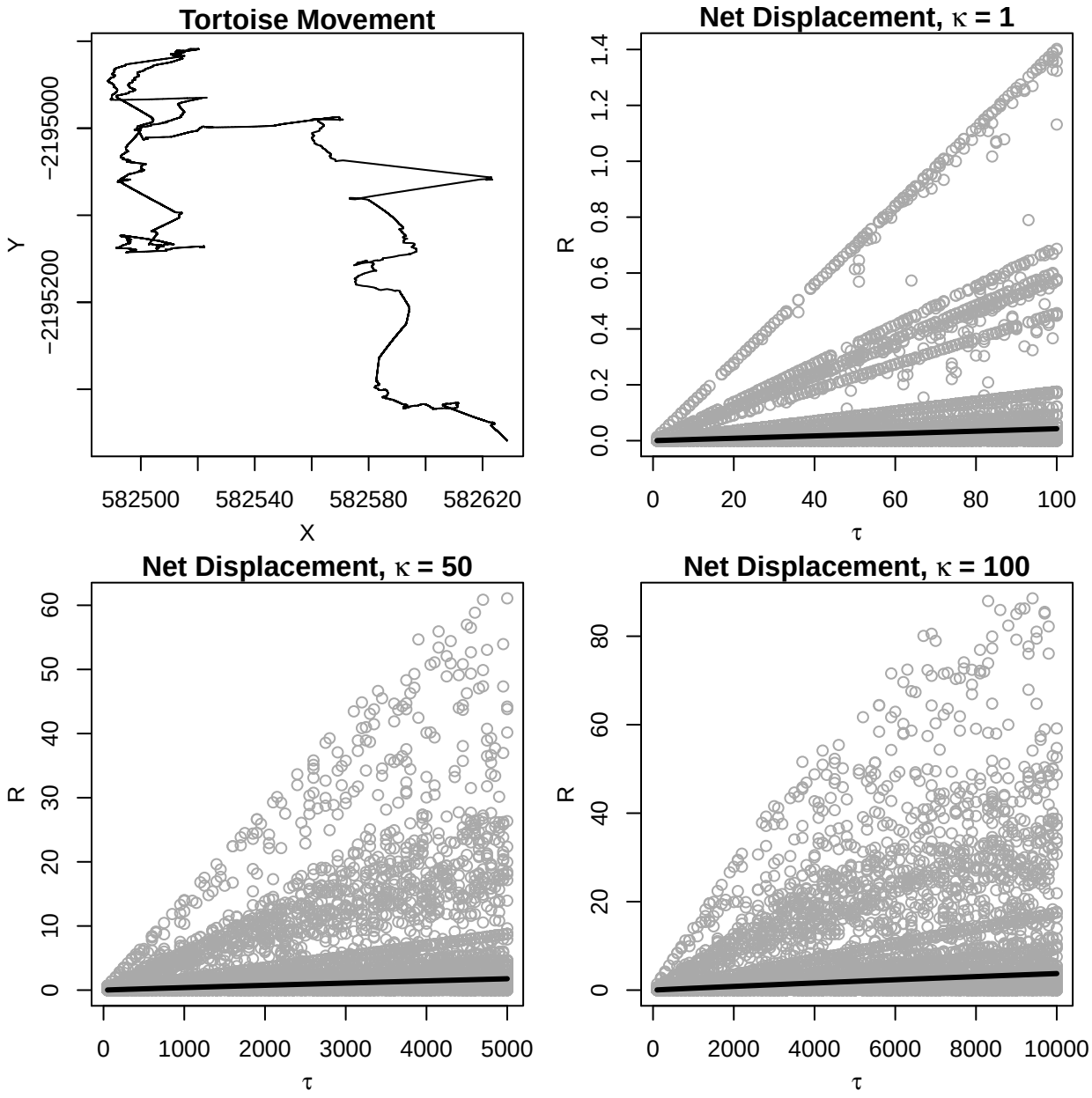
Tortoise Movement
Y
−2195000
−2195200
582500
582540
582580
582620
X
Net Displacement, κ = 1
R
0.0
0.2
0.4
0.6
0.8
1.0
1.2
1.4
0
20
40
60
80
100
τ
Net Displacement, κ = 50
R
0
10
20
30
40
50
60
0
1000
2000
3000
4000
5000
τ
Net Displacement, κ = 100
R
0
20
40
60
80
0
2000
4000
6000
8000
10000
τ

Figure 5

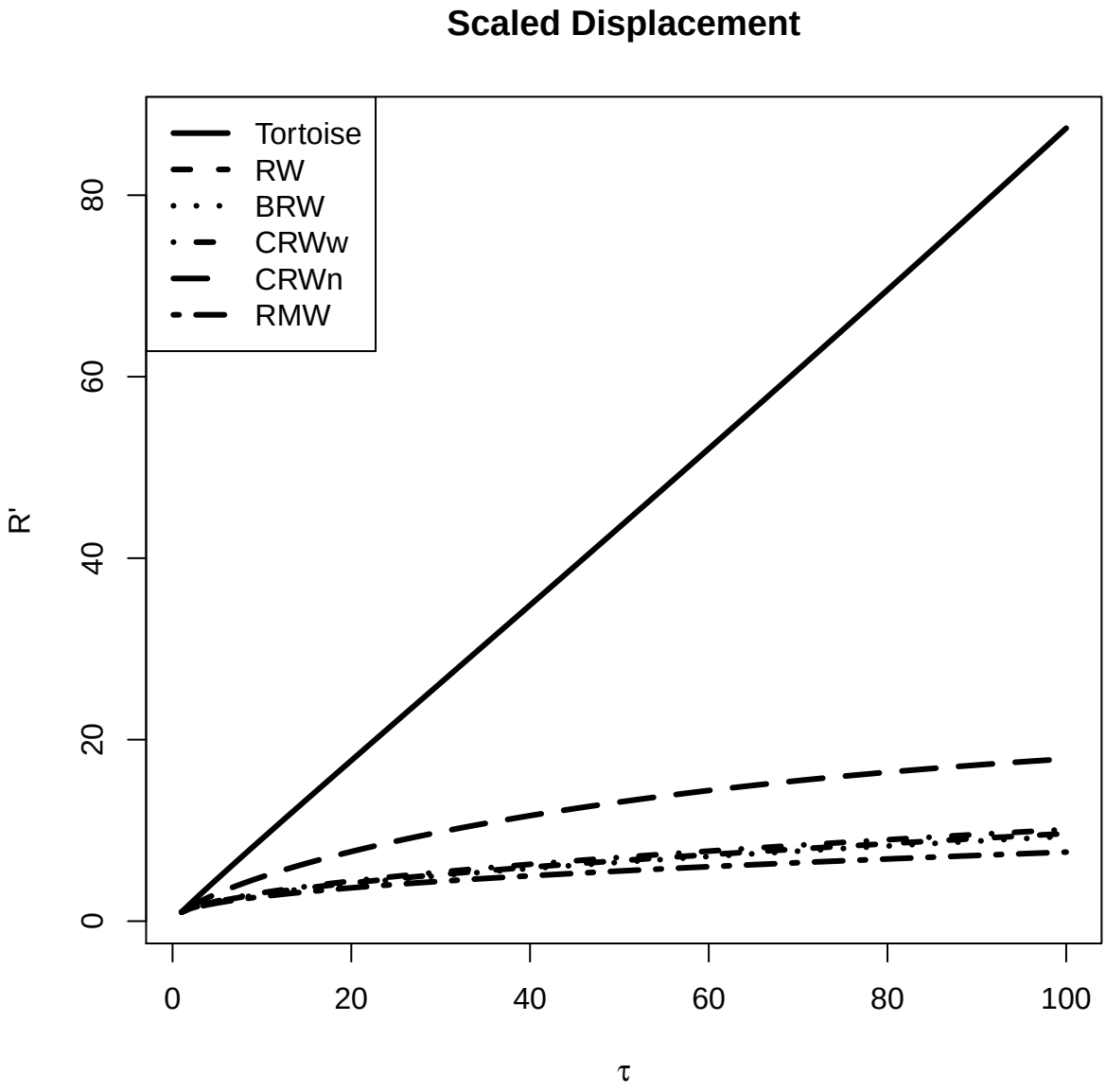
Scaled Displacement
Tortoise
RW
BRW
CRWw
CRWn
RMW
R'
0
20
40
60
80
100
τ

Figure 6

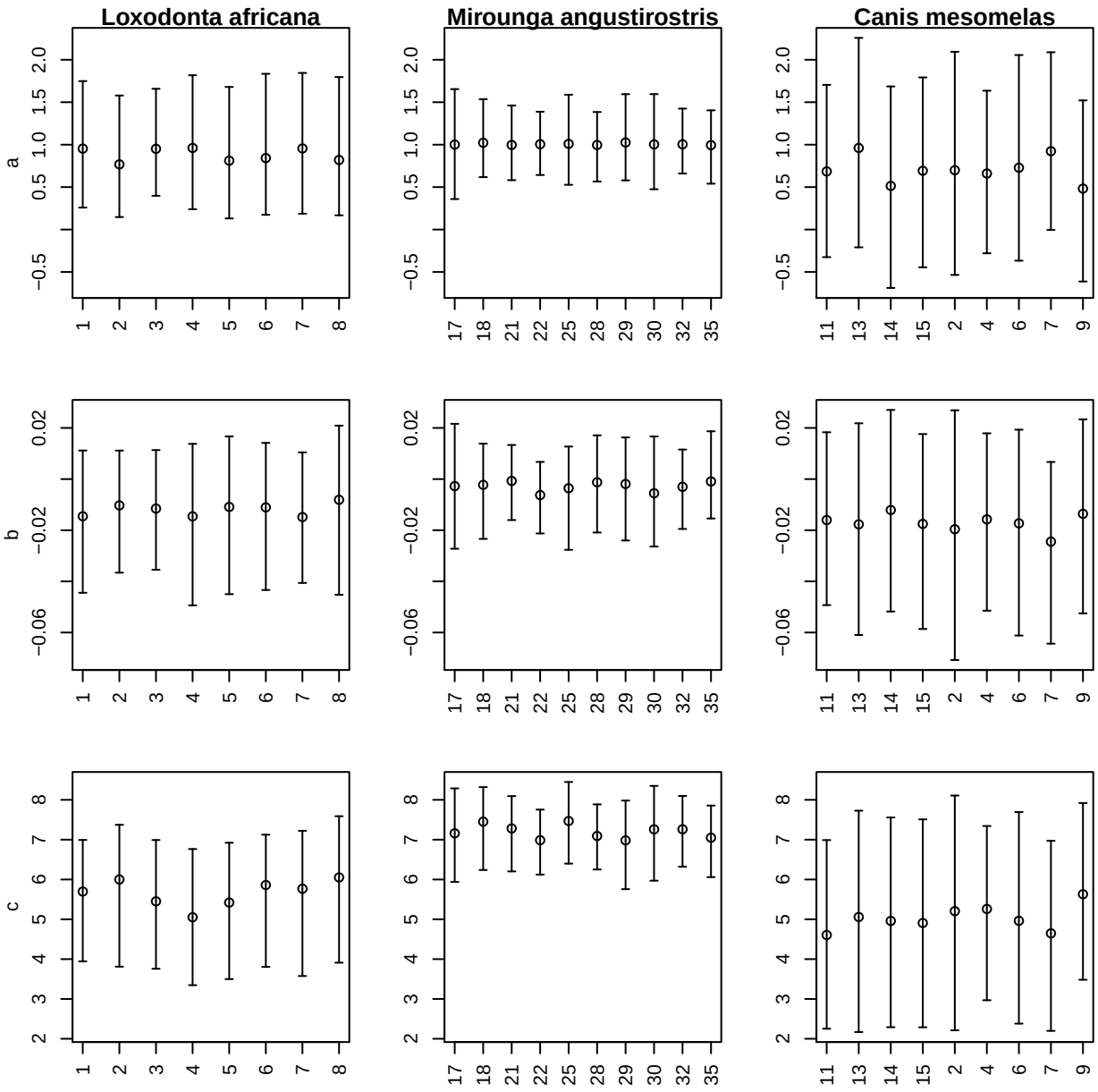
Loxodonta africana
Mirounga angustirostris
Canis mesomelas
a
b
c

654

Figure 7

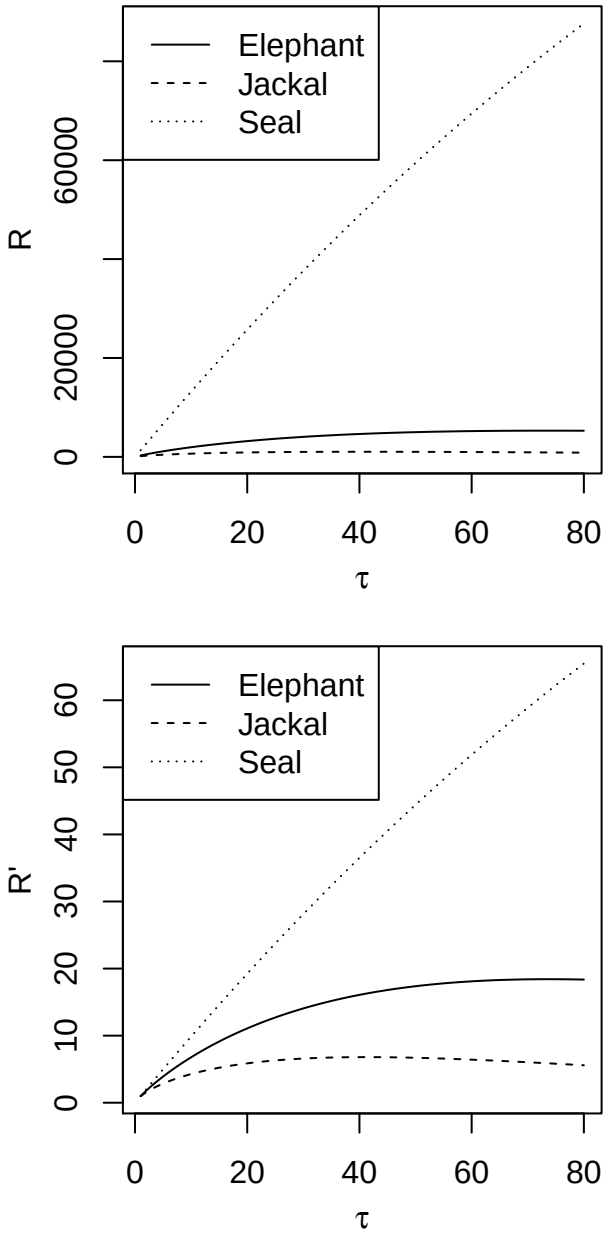
Elephant
Jackal
Seal
R
0
20000
60000
0
20
40
60
80
τ
Elephant
Jackal
Seal
R'
0
10
20
30
40
50
60
0
20
40
60
80
τ

Online Supporting Information

Appendix S1: Supplemental Figures

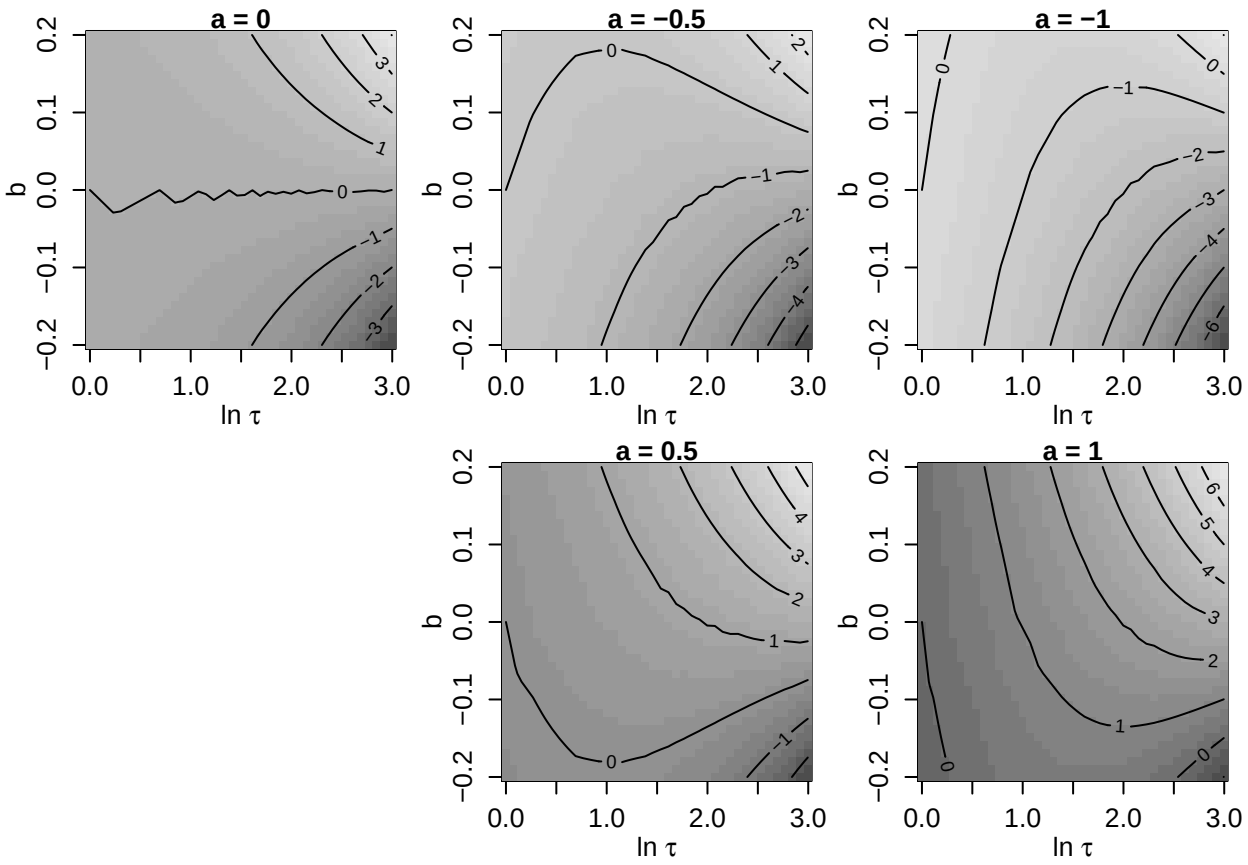

Figure S1: Variation in the natural logarithm of net displacement (R) as a function of a, b, and the natural logarithm of the time between successive relocations (τ) following the functional form $\ln R = a \ln \tau + b\tau + c$ and assuming $c = 0$. The parameter a is the slope of the log-linear relationship between R and τ, and b the skewness of the slope as a function of τ.

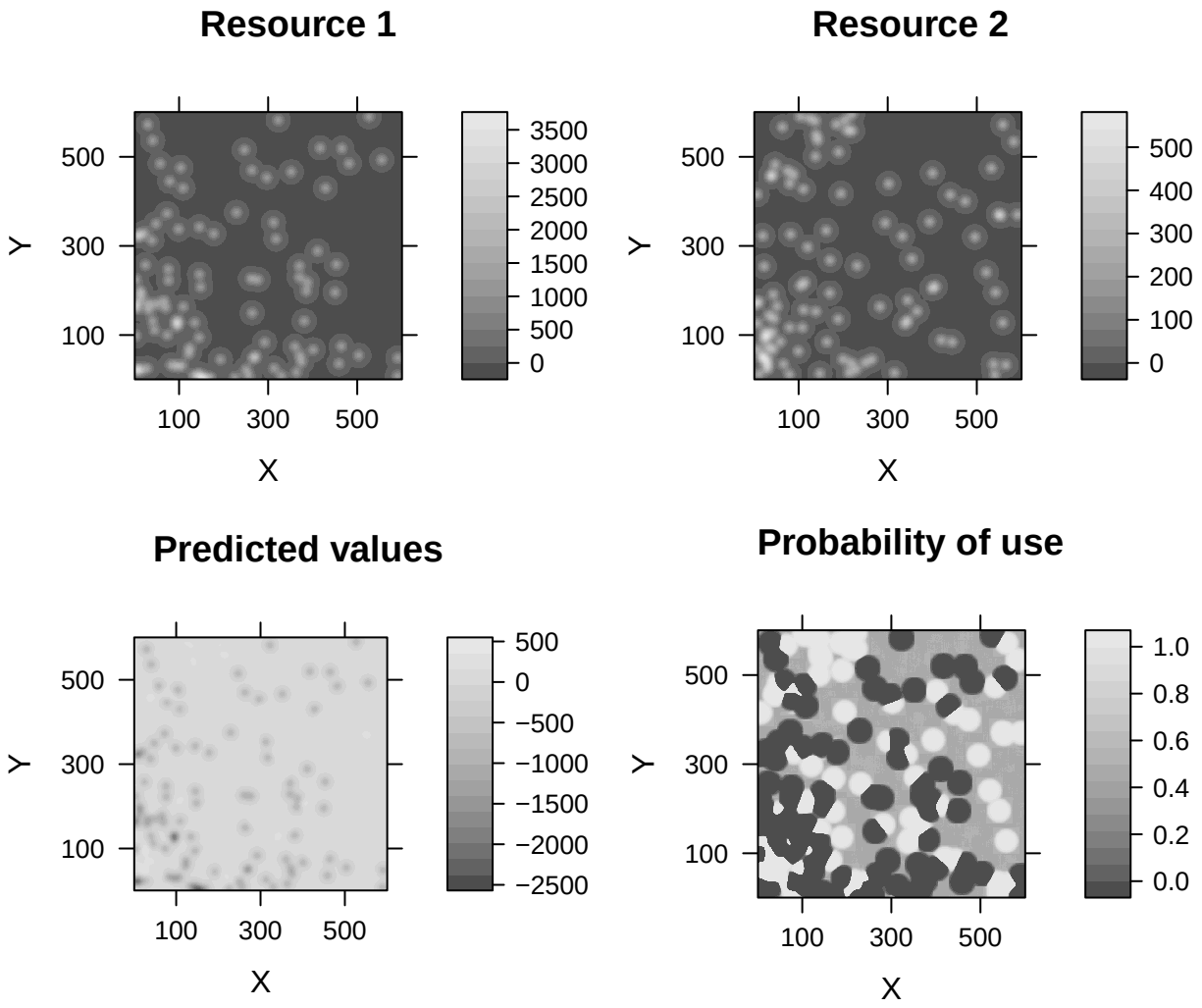

Figure S2: Simulated landscape of two resources in a 600 x 600 cell arena. Predicted values are generated from a hypothetical Resource Selection Function ($\hat{Y} = 0.5X_1 + 2X_2$). Probabilities are the inverse-logit of the predicted values.

Appendix S2: Simulating Movement Trajectories

```
#define step length and number of steps
step<-1
n<-1000000

##################
# simulate a RW #
##################

#set the random seed for consistent results
set.seed(1)

#define the turn angle distribution and calculate step deviations
theta.rw<-runif(n,0,2*pi)
theta.rw<-cumsum(theta.rw)
dx.rw<-step*cos(theta.rw)
dy.rw<-step*sin(theta.rw)

#calculate the observed random steps
x.rw<-cumsum(dx.rw)
y.rw<-cumsum(dy.rw)

plot(x.rw,y.rw,type="l")

############################################################
# simulate a CRW with narrow dispersion in turn angles #
############################################################

#call the circular library for the wrapped Cauchy distribution
```

```
library(circular)

#set the random seed for consistent results
set.seed(1)

#define the turn angle distribution and calculate step deviations
theta.crw<-rwrappedcauchy(n,mu=circular(0),rho=.8)
theta.crw<-cumsum(theta.crw)
dx.crw<-step*cos(theta.crw)
dy.crw<-step*sin(theta.crw)

#calculate the observed random steps
x.crw<-cumsum(dx.crw)
y.crw<-cumsum(dy.crw)
x.narrow<-x.crw
y.narrow<-y.crw

plot(x.crw,y.crw,type="l")

##########################################################
# simulate a CRW with wider dispersion in turn angles #
##########################################################

#set the random seed for consistent results
set.seed(1)

#define the turn angle distribution and calculate step deviations
theta.crw<-rwrappedcauchy(n,mu=circular(0),rho=.2)
theta.crw<-cumsum(theta.crw)
dx.crw<-step*cos(theta.crw)
```

```
dy.crw<-step*sin(theta.crw)

#calculate the observed random steps
x.crw<-cumsum(dx.crw)
y.crw<-cumsum(dy.crw)

plot(x.crw,y.crw,type="l")

###################
# simulate a BRW #
###################

#call the CircStats library
library(CircStats)

#define the storage array and define a starting location
n<-1000000
xy<-array(NA,c(n,2))
xy[1,]<-0

#set the random seed for consistent results
set.seed(1)

#generate random wrapped Cauchy deviates from 0
theta<-rwrpcauchy(n,location=0,rho=0.01)
theta[theta>pi]<-theta[theta>pi]-(2*pi)

#iterate over n steps
for(i in 1:(n-1)){
  #calculate heading towards [0,0] relative to x-axis
```

```
  alpha<-atan2(xy[i,2],xy[i,1])-pi
  #update xy position
  xy[i+1,]<-c((xy[i,1]+cos(alpha+theta[i])),(xy[i,2]+sin(alpha+theta[i])))
}

plot(xy,type="l")

library(CircStats)

#####################
#                   #
# for composite CRW #
#                   #
#####################

rm(list=ls(all=TRUE))
n <- 1000000

#the x-position of one of the attactors; the y-position is 0 and the other attarctor is at [-x.attracto
x.attractor <- 1000

xy <- array(NA,c(n,2))
xy[1,] <- c(-x.attractor,0)

#define a vector of movement modes
duration.min.t <- 2000
duration.max.t <- 2200 #adjust this value according to rho for mode t
duration.min.f <- 9000
duration.max.f <- 11000
mode <- vector()
```

```
while(length(mode)<n){
  mode <- c(mode, rep(TRUE, duration.min.t+(runif(1)*(duration.max.t-duration.min.t))))
  mode <- c(mode, rep(FALSE, duration.min.f+(runif(1)*(duration.max.f-duration.min.f))))
}
mode <- mode[1:n]

#generate random wrapped Cauchy deviates from 0
set.seed(1)
theta <- vector(length=n)
theta[mode] <- rwrpcauchy(sum(mode),location=0,rho=0.9)
theta[!mode] <- rwrpcauchy(sum(!mode),location=0,rho=0.1)
theta[theta>pi] <- theta[theta>pi]-(2*pi)

#iterate over n steps
heading <- runif(1,0,2*pi)
for(i in 2:n){
  heading <- heading+theta[i]
  #update xy position
  xy[i,] <- c((xy[i-1,1]+cos(heading)),(xy[i-1,2]+sin(heading)))
}

plot(xy, type="l")
write.csv(xy,"C:\\Users\\gstreet\\Documents\\Manuscripts\\Allometry of Net Displacement\\Data\\Revision

#######################################
#                                     #
# for CRW within the sedentary range  #
#                                     #
#######################################
```

```
rm(list=ls(all=TRUE))
n <- 1000000

#the x-position of one of the attactors; the y-position is 0 and the other attarctor is at [-x.attracto
x.attractor <- 1000

xy <- array(NA,c(n,2))
xy[1,] <- c(-x.attractor,0)

#define a vector of movement modes
duration.min.t <- 2000
duration.max.t <- 2200 #adjust this value according to rho for mode t
duration.min.f <- 9000
duration.max.f <- 11000
mode <- vector()
while(length(mode)<n){
  mode <- c(mode, rep(TRUE, duration.min.t+(runif(1)*(duration.max.t-duration.min.t))))
  mode <- c(mode, rep(FALSE, duration.min.f+(runif(1)*(duration.max.f-duration.min.f))))
}
mode <- mode[1:n]

#generate random wrapped Cauchy deviates from 0
set.seed(1)
theta <- vector(length=n)
theta[mode] <- rwrpcauchy(sum(mode),location=0,rho=0.9)
theta[!mode] <- rwrpcauchy(sum(!mode),location=0,rho=0.1)
theta[theta>pi] <- theta[theta>pi]-(2*pi)

#iterate over n steps
heading <- runif(1,0,2*pi)
```

```
for(i in 2:n){
  if(mode[i]){ #'migratory'/'homing' mode
    if(!mode[i-1]){x.attractor <- -x.attractor} #switch attractor if shifting from sedentary mode
    alpha <- atan2(xy[(i-1),2],xy[(i-1),1]-x.attractor)-pi #calculate heading towards the attractor rela
    heading <- alpha+theta[i]
  }else{ #'sedentary'/'foraging' mode
    heading <- heading+theta[i] #CRW within the sedentary range
  }
  #update xy position
  xy[i,] <- c((xy[i-1,1]+cos(heading)),(xy[i-1,2]+sin(heading)))
}

plot(xy, type="l")
write.csv(xy,"C:\\Users\\gstreet\\Documents\\Manuscripts\\Allometry of Net Displacement\\Data\\Revision

########################################
#                                      #
# for BRW within the sedentary range #
#                                      #
########################################

rm(list=ls(all=TRUE))
n <- 1000000

#the x-position of one of the attactors; the y-position is 0 and the other attarctor is at [-x.attracto
x.attractor <- 1000

xy <- array(NA,c(n,2))
xy[1,] <- c(-x.attractor,0)
```

```
#define a vector of movement modes
duration.min.t <- 2000
duration.max.t <- 2200 #adjust this value according to rho for mode t
duration.min.f <- 9000
duration.max.f <- 11000
mode <- vector()
while(length(mode)<n){
  mode <- c(mode, rep(TRUE, duration.min.t+(runif(1)*(duration.max.t-duration.min.t))))
  mode <- c(mode, rep(FALSE, duration.min.f+(runif(1)*(duration.max.f-duration.min.f))))
}
mode <- mode[1:n]

#generate random wrapped Cauchy deviates from 0
set.seed(1)
theta <- vector(length=n)
theta[mode] <- rwrpcauchy(sum(mode),location=0,rho=0.9)
theta[!mode] <- rwrpcauchy(sum(!mode),location=0,rho=0.1)
theta[theta>pi] <- theta[theta>pi]-(2*pi)

#iterate over n steps
heading <- runif(1,0,2*pi)
for(i in 2:n){
  if(mode[i]){ #'migratory'/'homing' mode
    if(!mode[i-1]){x.attractor <- -x.attractor} #switch attractor if shifting from sedentary mode
    alpha <- atan2(xy[(i-1),2],xy[(i-1),1]-x.attractor)-pi #calculate heading towards the attractor rela
    heading <- alpha+theta[i]
  }else{ #'sedentary'/'foraging' mode
    alpha <- atan2(xy[(i-1),2],xy[(i-1),1]-x.attractor)-pi
    heading <- alpha+theta[i]
  }
```

```
  #update xy position
  xy[i,] <- c((xy[i-1,1]+cos(heading)),(xy[i-1,2]+sin(heading)))
}

plot(xy, type="l")
write.csv(xy,"C:\\Users\\gstreet\\Documents\\Manuscripts\\Allometry of Net Displacement\\Data\\Revision

##############################
#                            #
# for Central Place Foraging #
#                            #
##############################

rm(list=ls(all=TRUE))
n <- 1000000

#the x-position of one of the attactors; the y-position is 0 and the other attractor is at [-x.attracto
x.attractor <- 0

xy <- array(NA,c(n,2))
xy[1,] <- c(-x.attractor,0)

#define a vector of movement modes
duration.min.t <- 2000
duration.max.t <- 2200 #adjust this value according to rho for mode t
duration.min.f <- 9000
duration.max.f <- 11000
mode <- vector()
while(length(mode)<n){
  mode <- c(mode, rep(TRUE, duration.min.t+(runif(1)*(duration.max.t-duration.min.t))))
```

```
  mode <- c(mode, rep(FALSE, duration.min.f+(runif(1)*(duration.max.f-duration.min.f))))
}
mode <- mode[1:n]

#generate random wrapped Cauchy deviates from 0
set.seed(1)
theta <- vector(length=n)
theta[mode] <- rwrpcauchy(sum(mode),location=0,rho=0.9)
theta[!mode] <- rwrpcauchy(sum(!mode),location=0,rho=0.1)
theta[theta>pi] <- theta[theta>pi]-(2*pi)

#iterate over n steps
heading <- runif(1,0,2*pi)
for(i in 2:n){
  if(mode[i]){ #'migratory'/'homing' mode
    if(!mode[i-1]){x.attractor <- -x.attractor} #switch attractor if shifting from sedentary mode
    alpha <- atan2(xy[(i-1),2],xy[(i-1),1]-x.attractor)-pi #calculate heading towards the attractor rela
    heading <- alpha+theta[i]
  }else{ #'sedentary'/'foraging' mode
    alpha <- atan2(-xy[(i-1),2],-xy[(i-1),1])-pi
    heading <- alpha+theta[i]
  }
  #update xy position
  xy[i,] <- c((xy[i-1,1]+cos(heading)),(xy[i-1,2]+sin(heading)))
}

plot(xy, type="l")
write.csv(xy,"C:\\Users\\gstreet\\Documents\\Manuscripts\\Allometry of Net Displacement\\Data\\Revision
```

Appendix S3: Simulating a Landscape and RMW

```
library(KernSmooth)
library(lattice)
library(gridExtra)

lattice.options(default.theme = standard.theme(color = FALSE))

##############################################################################################
#                                                                                            #
# the function to generate the landscape, from Matthiopoulos et al. 2015, EcolMono           #
#                                                                                            #
##############################################################################################
environ<-function(d,x,mx,bw,sl)
{
  ar<-array(0, dim=c(d,d))
  # Places seeds in arena
  slope<- sl # 0.05 # Introduces SW-to-NE gradient in resource
  cox<-cbind(1+(d-1)*runif(x, min=0, max=1)^slope, 1+(d-1)*runif(x, min=0, max=1)^slope)
  # Smooths seeds to create spatial autocorrelation
  sarx<-bkde2D(cox, bandwidth = c(bw,bw), gridsize=c(d,d),range.x=list(c(1,d),c(1,d)))
  ii<-rep(1:d,d)
  jj<-rep(1:d, each=d)

  sarx$fhat<-mx*(sarx$fhat/mean(sarx$fhat))
  return(sarx$fhat)
}

##############################################################################
#                                                                            #
```

```
# generate the landscape of covariates, from Matthiopoulos et al. 2015 #
#                                                                      #
########################################################################

set.seed(1)
d<-600  #  Arena dimensions
smooth_scaler<-8 #scaling coefficient for bandwidth

x1<-round(runif(1,100,100))  # Number of resource 1 distribution foci
x2<-round(runif(1,5,10))   # Number of resource 2 distribution foci
mx1<-runif(1,100,200)  # Average amount of resource 1 across arena
mx2<-runif(1,26,27)   # Average value of resource 2 across arena
bw1<-smooth_scaler+rexp(1,1/4) # Smoothing bandwidth for generation of environmental layers
sl1<-runif(1,0.5,2) # Geographical gradient in distribution of resource 1
sl2<-runif(1,0.5,2) # Geographical gradient in distribution of resource 2
env1<-environ(d,x1,mx1,bw1,sl1)  # Generation of resource 1 layer
env2<-environ(d,x1, mx2,bw1,sl2)  # Generation of resource 2 layer
env1.plot<-levelplot(env1,xlab="X",ylab="Y",main="Resource 1",
                     scales=list(x=list(at=c(100, 300, 500)),
                     y=list(at=c(100, 300, 500))))
env2.plot<-levelplot(env2,xlab="X",ylab="Y",main="Resource 2",
                     scales=list(x=list(at=c(100, 300, 500)),
                     y=list(at=c(100, 300, 500))))

#####################################
#                                   #
# generate the landscape of fitness #
#                                   #
#####################################
```

```
a1<-log(0.5) # RSF coefficient for resource 1
a2<-log(2) # RSF coefficient for resource 2
fitinit<-a1*env1+a2*env2  # Solution of the RSF over space
fitinit.plot<-levelplot(fitinit,xlab="X",ylab="Y",main="Predicted values",
                        scales=list(x=list(at=c(100, 300, 500)),
                        y=list(at=c(100, 300, 500))))

prob<-exp(fitinit)/(1+exp(fitinit)) #convert to probability based on RSF
prob.plot<-levelplot(prob,xlab="X",ylab="Y",main="Probability of use",
                     scales=list(x=list(at=c(100, 300, 500)),
                     y=list(at=c(100, 300, 500))))

grid.arrange(env1.plot,env2.plot,fitinit.plot,prob.plot,ncol=2)

###################################
#                                 #
# Simulate movement on landscape #
#                                 #
###################################

#set the random seet for consistent results
set.seed(1)

len<-1000000 #number of model iterations to run
x<-numeric(len) #parameterize the x and y coordinate data
y<-numeric(len)
x[1]<-round(runif(1,1,d),0) #specify starting x and y coordinates
y[1]<-round(runif(1,1,d),0)

r<-2 #specify the Manhattan distance
```

```
x_vN<-seq(-r,r,1) #populate x and y differentials based on Manhattan distance
y_vN<-seq(-r,r,1)
vN_pos<-expand.grid(x_vN,y_vN) #get all combinations of the x and y differentials
vN_pos<-vN_pos[which(abs(vN_pos$Var1)+abs(vN_pos$Var2) <= r),] #keep only those rows
#where the sum of the absolute values is less than or equal to r
names(vN_pos)<-c("x","y")

for(i in 2:len)
{
  #identify the von Neumann neighborhood around the animal assuming r = 2
  vNn<-data.frame(vN_pos$x + x[i-1], vN_pos$y + y[i-1])
  names(vNn)<-c("x","y")
  #exclude any locations exceeding the arena limits (i.e., <=1 or >=d)
  vNn<-vNn[vNn$x >= 1 & vNn$x <= d & vNn$y >= 1 & vNn$y <= d,]
  #pull the probability values from the probability landscape
  vNn_prob<-numeric(length(vNn$x))
  for(j in 1:length(vNn$x))
  {
    vNn_prob[j]<-prob[vNn$x[j],vNn$y[j]]
  }
  #select one of the cells with probability equal to the scaled probability
  vNn_prob<-vNn_prob/sum(vNn_prob)
  sel<-sample(1:length(vNn_prob),1,prob=vNn_prob)
  #store the coordinates of the selected cell
  x[i]<-vNn$x[sel]
  y[i]<-vNn$y[sel]
}

pos<-data.frame(x,y)
plot(pos,xlim=c(0,d),ylim=c(0,d),type="l",xlab="X",ylab="Y",main="Resource-mediated walk")
```

Appendix S4: Bootstrap Protocol for RW Model Only

```
#load libraries
library(reshape2)

#how many time intervals do you want to plot for?
tau_max<-100

#parameters for a matrix to store the data following the bootstrap
#define the columns
dt<-seq(1,tau_max,1)
#define the rows (i.e., the number of bootstrap iterations)
nboot<-100

#set the random seed
set.seed(1)

#read in the data for a random walk
rw<-read.csv("rw.csv")

#create the matrix
data.rw<-matrix(NA,ncol=length(dt),nrow=nboot)

#start the bootstrap!
#the i loop is the bootstrap iterator
for(i in 1:nboot)
{
  #which fixes are allowable (i.e., to prevent resampling of fixes, or sampling fixes
  #between two previous selected fixes, and thus ensuring independence)
  allow<-seq(1,length(rw[,1]),1)
```

```
1107
      #the j loop is the in-sample iterator
      #going backward to increase loop efficiency
1110  for(j in length(dt):1)
      {
        #pick a starting point for the time interval
1113    #repeat until the start point: 1) is not associated with an end point outside of the
        #observations, and 2) produces fixes that are still allowable (i.e., that haven't already
        #been sampled)
1116    repeat{
          temp<-sample(seq(1,length(rw[,1])),1)
          if(temp+dt[j]<=length(rw[,1]) & all(seq(temp,temp+dt[j],1) %in% allow)){
1119        break
          }
        }
1122
        #calculate and store the displacement between the start and end point based on that dt
        #value
1125    data.rw[i,j]<-sqrt(((rw[temp+dt[j],1]-rw[temp,1])^2)+((rw[temp+dt[j],2]-rw[temp,2])^2))
        #mark those fixes, and all between them, as being unallowed
        allow<-allow[-which(allow %in% seq(temp,temp+dt[j],1))]
1128  }
    }

1131 #transform the matrix to a vector
    colnames(data.rw)<-dt
    rownames(data.rw)<-chartr("1234567890","ABCDEFGHIJ",seq(1,nboot,1))
1134 rw.melt<-melt(data.rw)
    rw.melt<-rw.melt[,-1]
    colnames(rw.melt)<-c("dt","R")
```

```
##############################################
#                                            #
# Now run one model per bootstrap iteration  #
#                                            #
##############################################

#create the data matrices to store the model outputs
rw_coef<-data.frame(a=numeric(),b=numeric(),c=numeric(),R2=numeric())

#fit one model per bootstrap iteration
for(i in 1:nrow(data.rw))
{
  #extract the i-th bootstrapped sample
  rwR<-data.rw[i,]

  #run the model
  rw.mod<-lm(log(rwR[rwR>0])~log(dt[rwR>0])+dt[rwR>0])

  #save the relevant model outputs
  rw_coef<-rbind.data.frame(rw_coef,data.frame(a=coefficients(rw.mod)[2],
                                               b=coefficients(rw.mod)[3],
                                               c=coefficients(rw.mod)[1],
                                               R2=summary(rw.mod)$adj.r.square))
}
```